EGU21-478, https://doi.org/10.5194/egusphere-egu21-478, 2021

Geodynamic Tomography: Constraining Upper-Mantle Deformation Patterns from the Bayesian Inversion of Surface Waves

John Keith Magali[1],Thomas Bodin[1], Navid Hedjazian[1],
Henri Samuel[2], Suzanne Atkins[3]

[1]UCBL,CNRS, LGL-TPE, Université de Lyon, , 69622 Villeurbanne, France
[2]Institut de Physique du Globe de Paris, Université de Paris, CNRS, F-75005 Paris, France
[3]Laboratoire de Géologie, Ecole Normale Supérieure, PSL Res. Univ, 75005 Paris, France

Seismic anisotropy

Definition: Variations in elastic properties of a medium to propagation direction (e.g. azimuthal anisotropy) and polarization orientation (e.g. radial anisotropy).

- Originates from the net alignment of anisotropic minerals (crystallographic preferred orientation, CPO) due to mantle deformation.
- Present-day flow can be constrained by anisotropy.
- Can be observed with surface wave tomography.

Intrinsic origin (CPO):

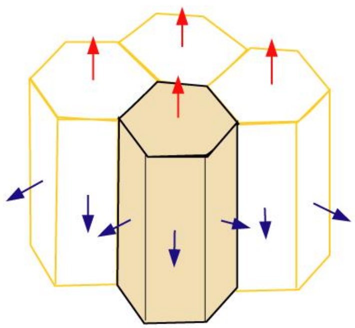

Net alignment of anisotropic crystals in rock-forming minerals

(e.g. Olivine)

May infer circulation patterns:

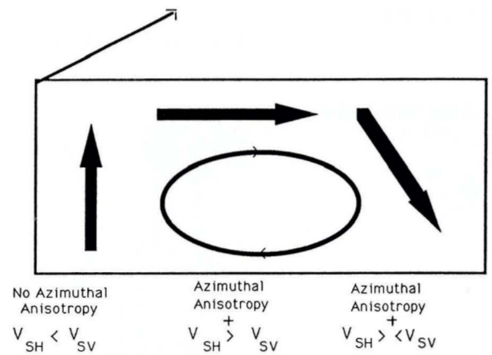

Montagner, 1994

(Over)simplified rule of thumb:

→ $V_{SH} > V_{SV}$: horizontal flow

→ $V_{SV} > V_{SH}$: vertical flow

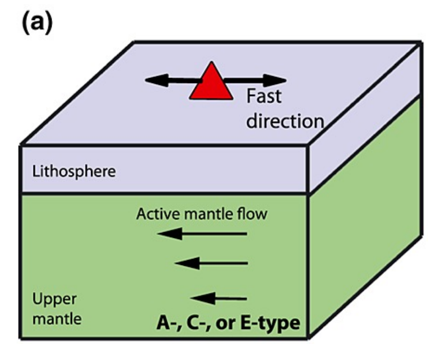

Olivine A-type

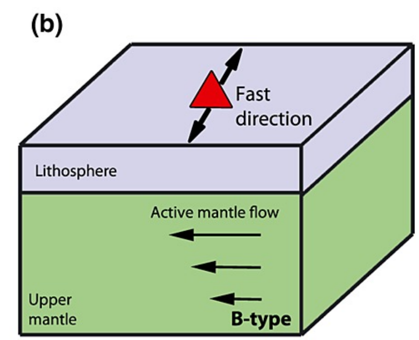

Olivine B-type

Long and Becker, 2010

Challenges in the current field of study

1. Inability of surface waves to give the full picture.

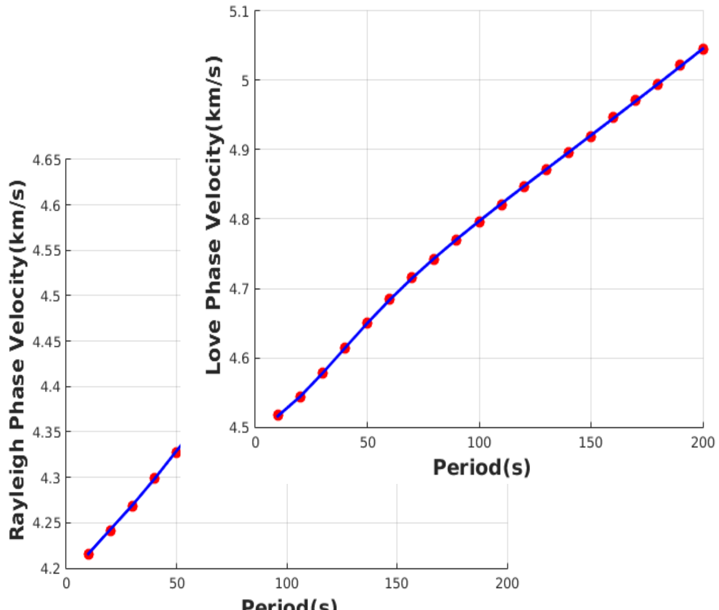

Dispersion measurements ($c_{R,}$ c_L, δc)

Inversion procedure

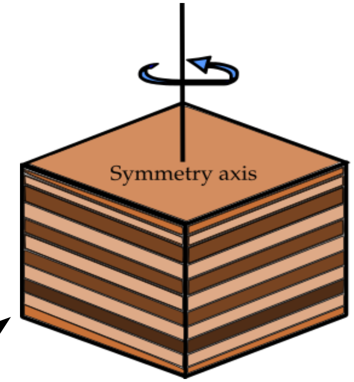

VTI (Radial anisotropy)

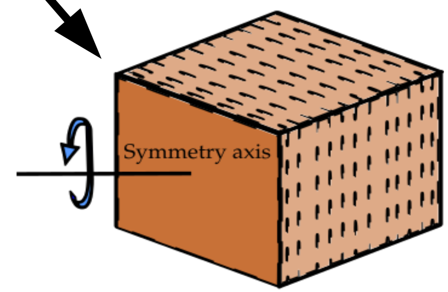

HTI (Azimuthal anisotropy)

Challenges in the current field of study

1. Inability of surface waves to give the full picture.

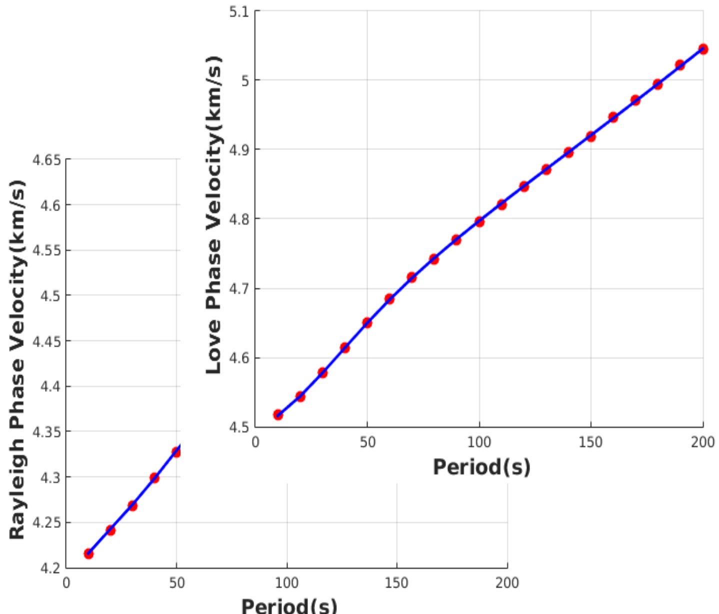

Dispersion measurements ($c_{R,}$ c_L, δc)

Inversion procedure ?

What we want is a dynamic view:

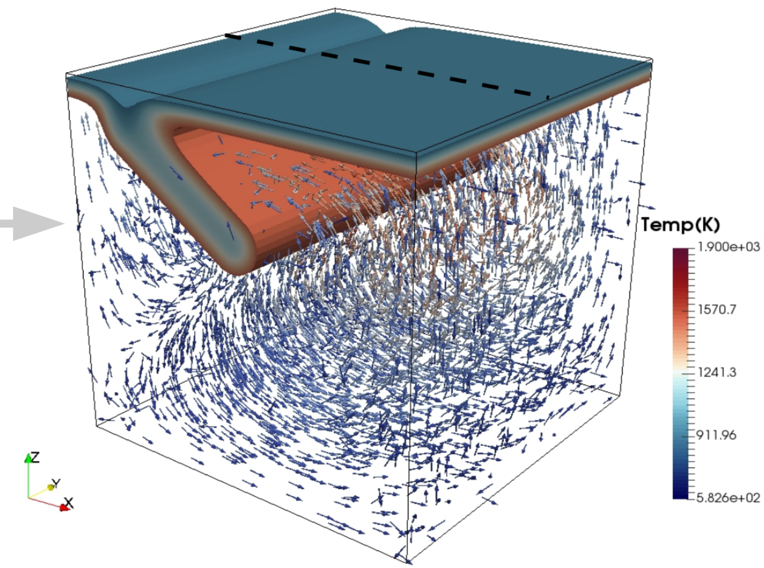

i.e., complete deformation patterns

Challenges in the current field of study

2. Limitations with parameterizations/High-dimensionality of anisotropic tomography.

$$S = \begin{pmatrix} S_{11} & S_{12} & S_{13} & S_{14} & S_{15} & S_{16} \\ S_{21} & S_{22} & S_{23} & S_{24} & S_{25} & S_{26} \\ S_{31} & S_{32} & S_{33} & S_{34} & S_{35} & S_{36} \\ S_{41} & S_{42} & S_{43} & S_{44} & S_{45} & S_{46} \\ S_{51} & S_{52} & S_{53} & S_{54} & S_{55} & S_{56} \\ S_{61} & S_{62} & S_{63} & S_{64} & S_{65} & S_{66} \end{pmatrix}$$

$\approx$

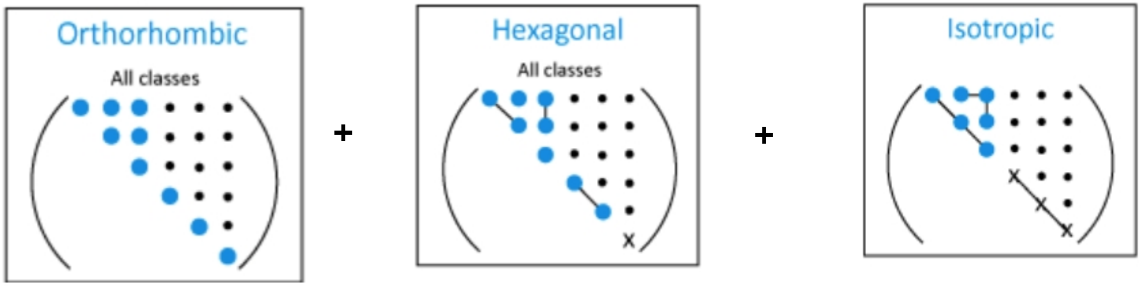

Surface waves are only sensitive to 13-depth functions of the elastic medium:

- Five for radial anisotropy
- Eight for azimuthal anisotropy

Challenges in the current field of study

3. Usage of non-data driven constraints.

Conventional tomography uses regularization that:

- May be non data-driven.
- Is dependent on ad-hoc choices.
- May bias uncertainty estimates.

Geodynamic tomography - a redefinition of the seismic imaging problem

A novel approach where no symmetry is imposed to the elastic tensor at the outset, and where seismic observations are inverted with constraints from geodynamic modeling and petrological modeling.

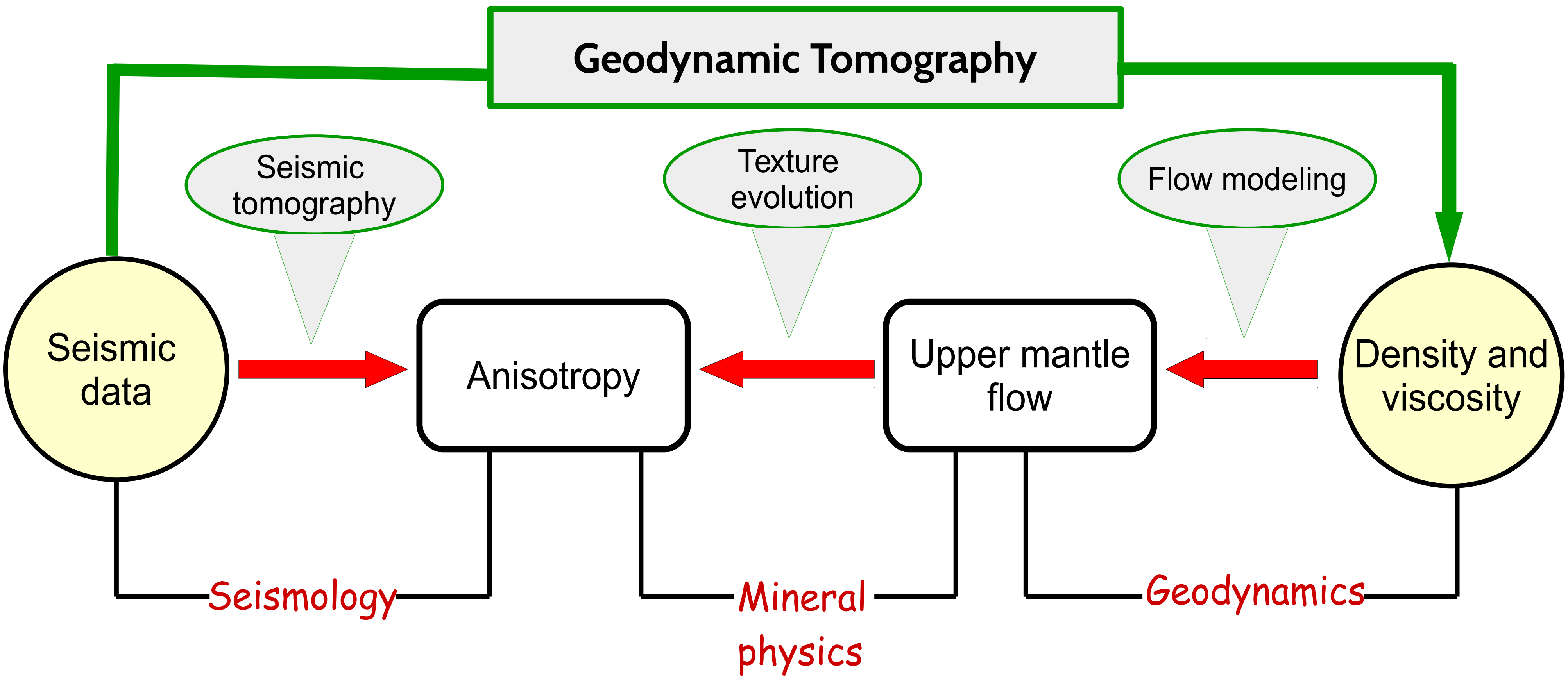

Joint geodynamic and seismic forward problem

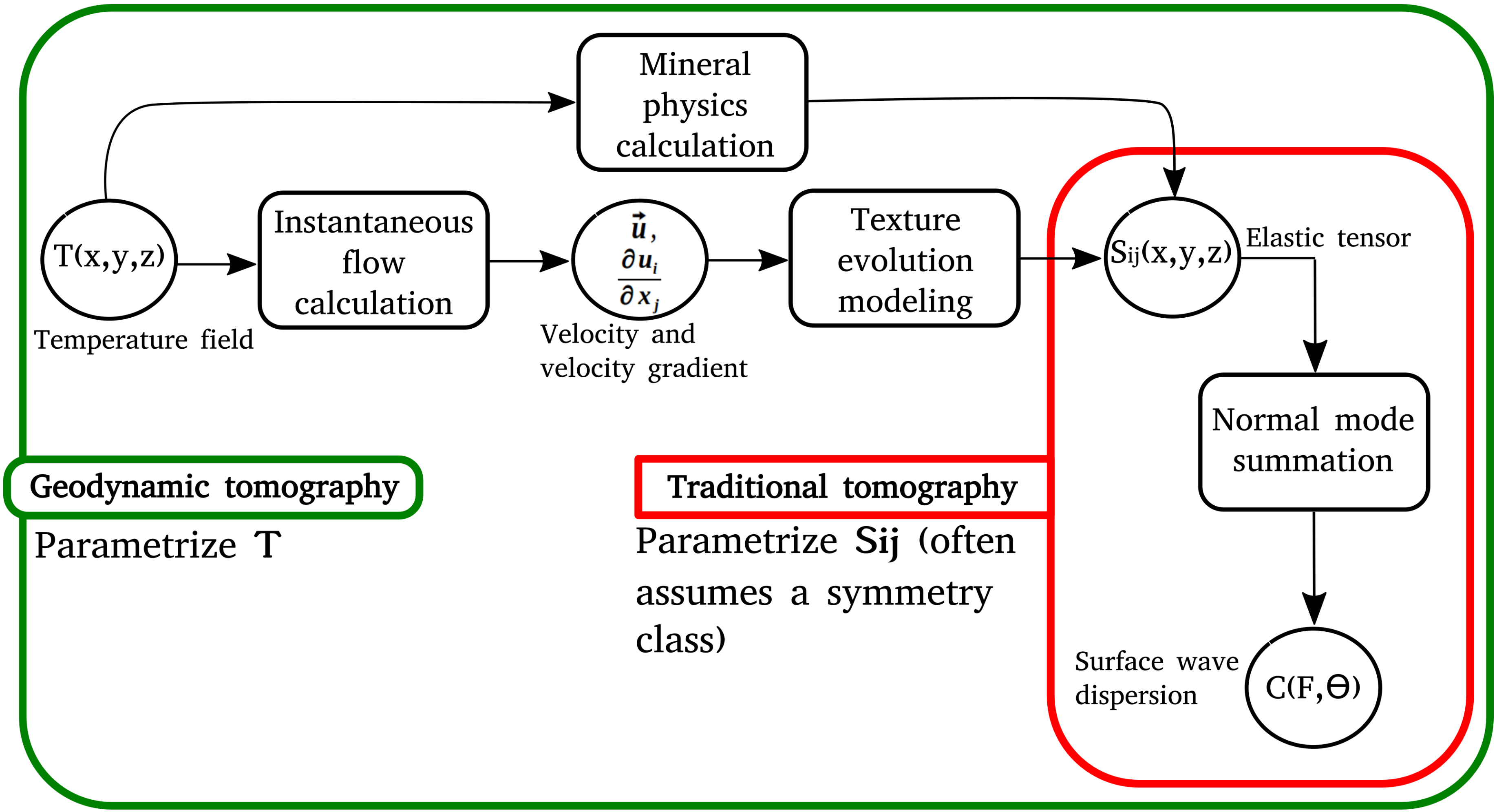

Joint geodynamic and seismic forward problem

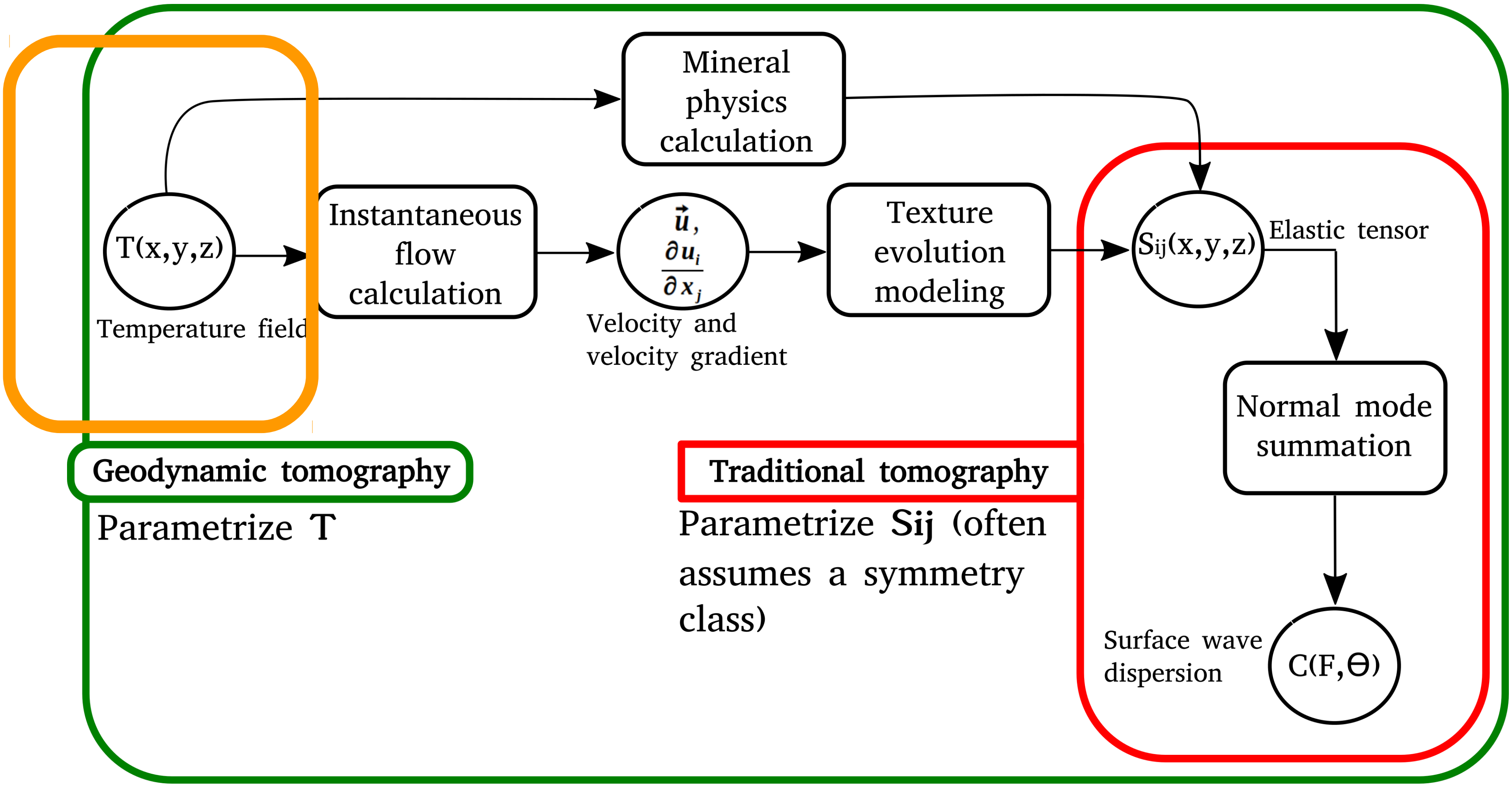

The model

- Temperature field T, activation energy for viscosity E.
- T depends on the number of spatial parameters (i.e. the grid size). Thus, if the entire volume is a 3-D cube, the total number of model parameters (including E) would be N^3+1.
- We introduce basis functions for T to further reduce the number of model parameters.

Example: A temperature field due to a single spherical anomaly

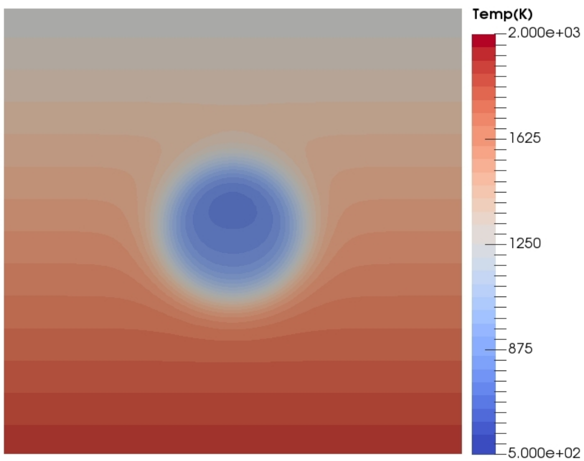

T can be written as:

$$T(\mathbf{r}) = T_{\text{background}}(\mathbf{r}) + \sum_{i=1}^{M} T^{i}_{\text{anomaly}}(\mathbf{r})$$

where a basis function for an anomaly can be expressed as:

$$T_{\text{anomaly}}(\mathbf{r}) = -\frac{T_c}{2}\left[1 - \tanh\left(\frac{\beta}{L_s}\left(\|\mathbf{r}-\mathbf{r_0}\| - \frac{R}{2}\right)\right)\right]$$

- We allow for lateral variations in viscosity. Here, we assume that viscosity follows an exponential law that depends on temperature:

$$\eta(\mathbf{r}) = \eta_0 \exp\left[-E\,\frac{(T(\mathbf{r}) - T_0)}{T_0}\right]$$

- In the inverse problem, E is treated as an unknown.

Unknown model parameters:

m = [T_c, R, x_0, y_0, z_0, E]

Joint geodynamic and seismic forward problem

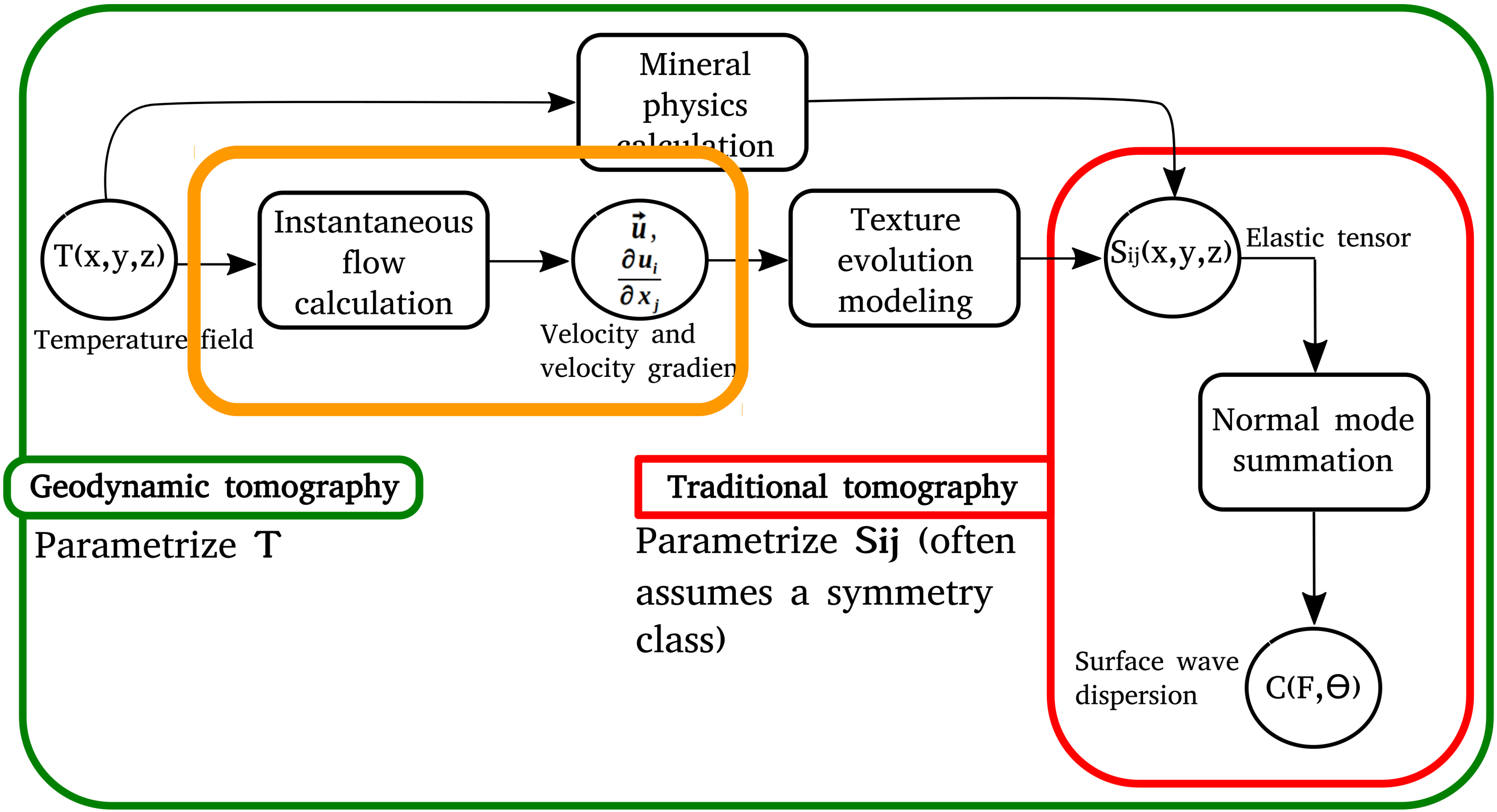

Modeling upper-mantle flow

- We consider the buoyancy-driven convection of a highly-viscous, Newtonian, and incompressible fluid in a 3-D Cartesian coordinate system.
- The flow is subjected to free-slip boundary conditions.

Governing equations:

- Mass conservation:
- Momentum conservation:

Inputs:

- Density. It is assumed to be a linear function of temperature.
- Viscosity.

Outputs:

- Velocity field.
- Velocity gradients.

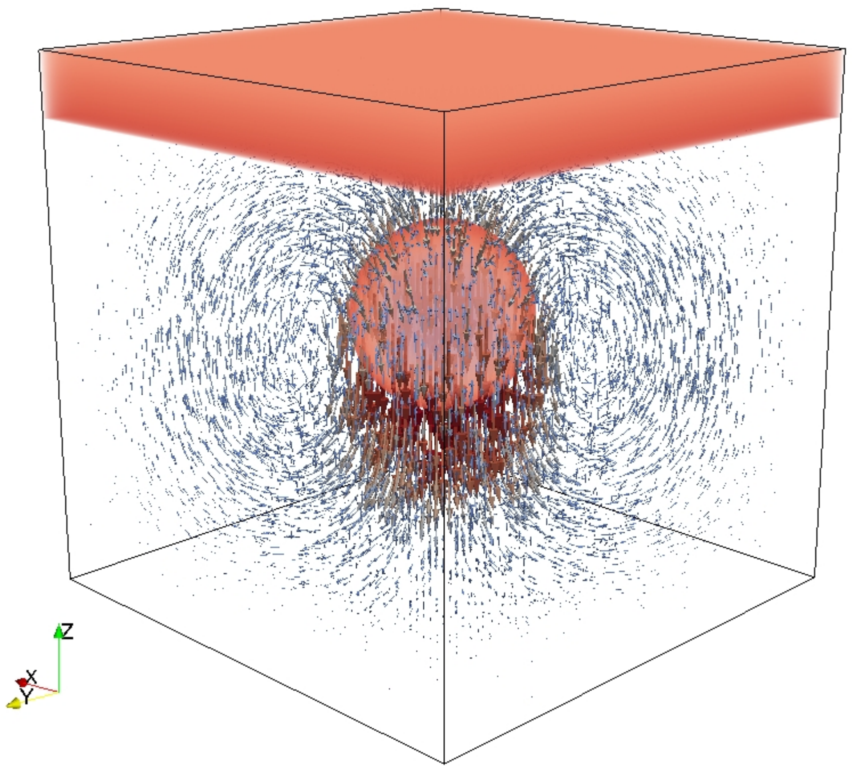

Example: instantaneous flow due to a sinking spherical anomaly.

Joint geodynamic and seismic forward problem

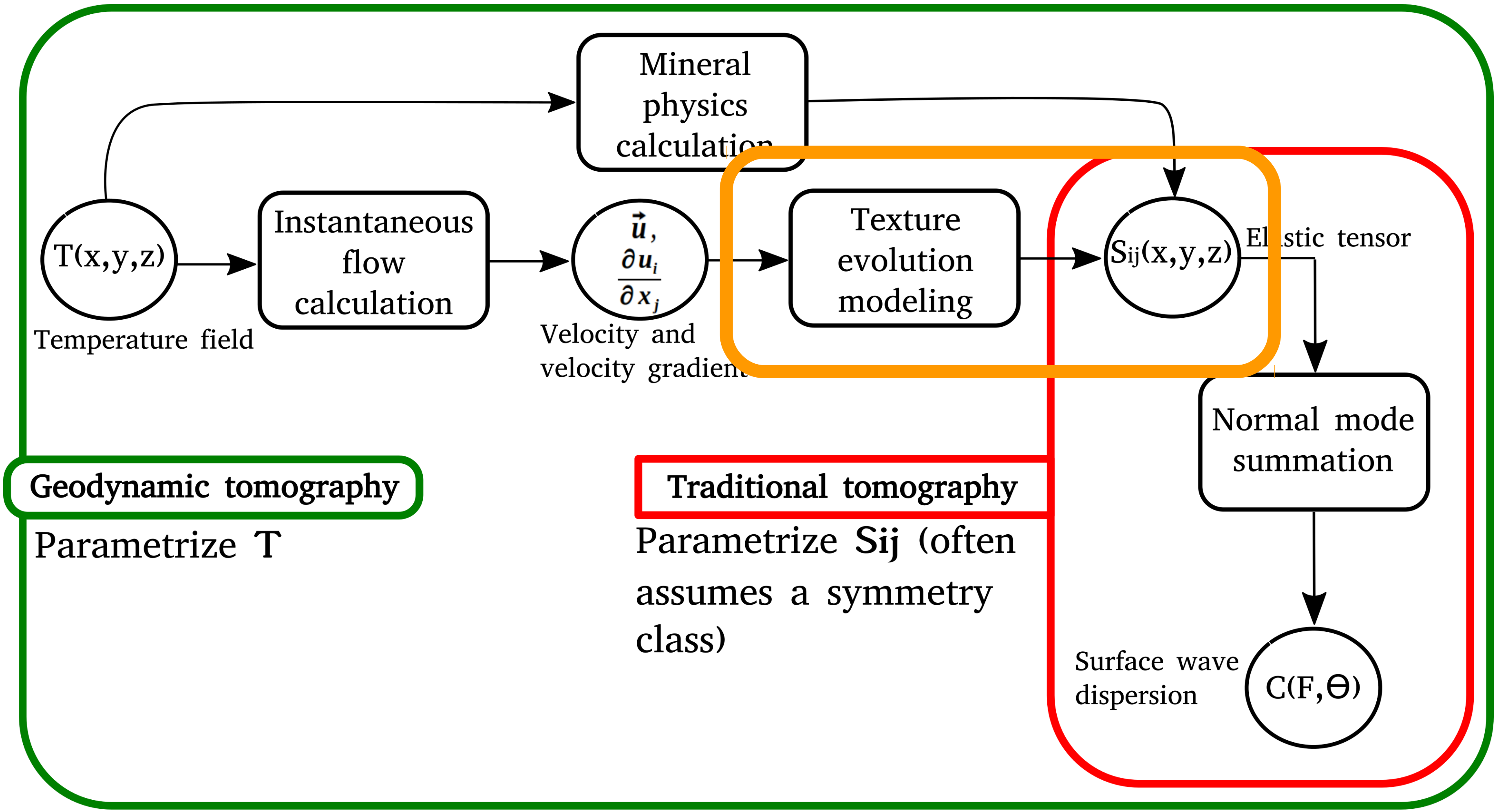

Micro-mechanical modeling of texture evolution

- Olivine aggregates deform under shear to form a Crystallographic Preferred Orientation (CPO).
- Full computation of anisotropy is required when (1) the strain field is complex, (2) CPO evolution is slower than changes in strain patterns.

Inputs:

- Velocity gradients.
- Mineralogic composition.
- Initial orientation of minerals.
- Control parameters for CPO evolution (usually constrained from experiments).

Method:

- **D-Rex,** a kinematic modeling of CPO that incorporates dynamic recrystallization (Kaminski, et al., 2004).

Output:

- Elastic tensor ***S***

Joint geodynamic and seismic forward problem

Fast-forward calculations of seismic anisotropy

Usage of computationally-expensive forward models are impractical when implemented in a sampling-based method, let alone, an inversion procedure.

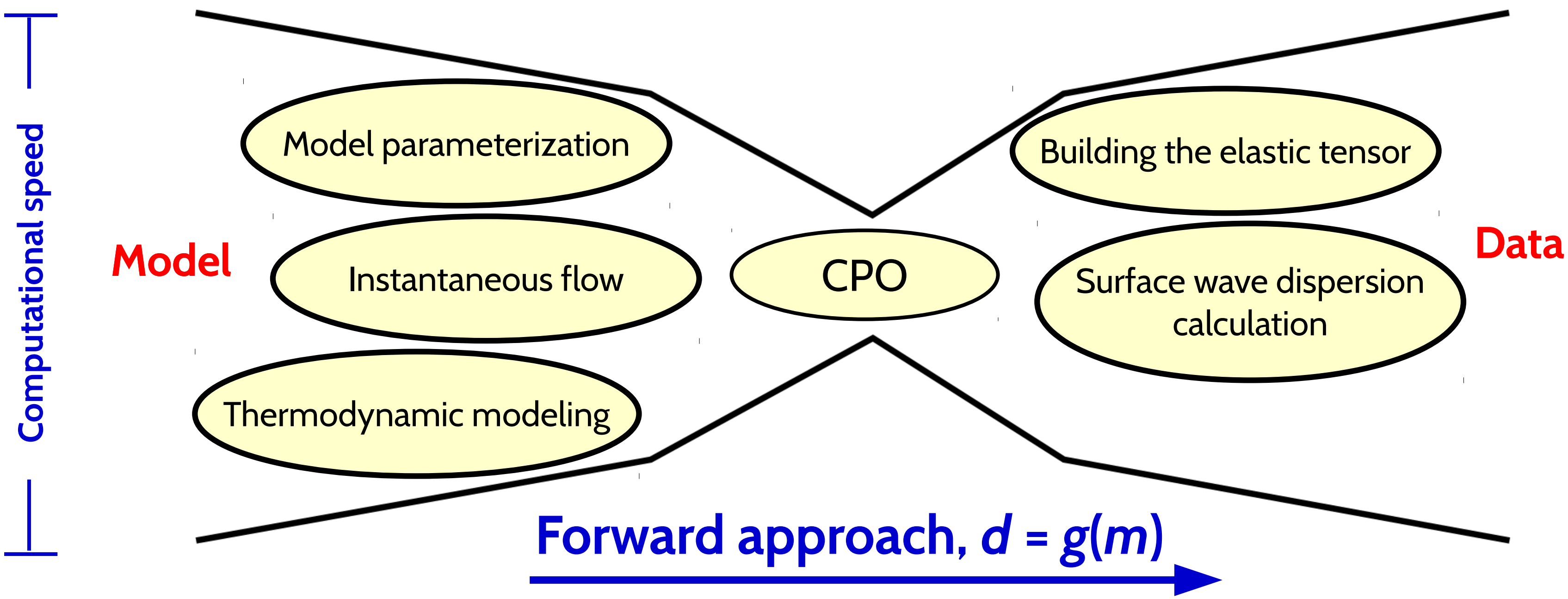

We fast-track the computation of the anisotropic component of the elastic tensor from velocity gradients with artificial neural networks (*Magali, et al., 2021*):

- The ANN is trained with family of convection models as training inputs and the anisotropic component as training outputs.
- The network is used as a surrogate model to D-Rex in the inversions.

Joint geodynamic and seismic forward problem

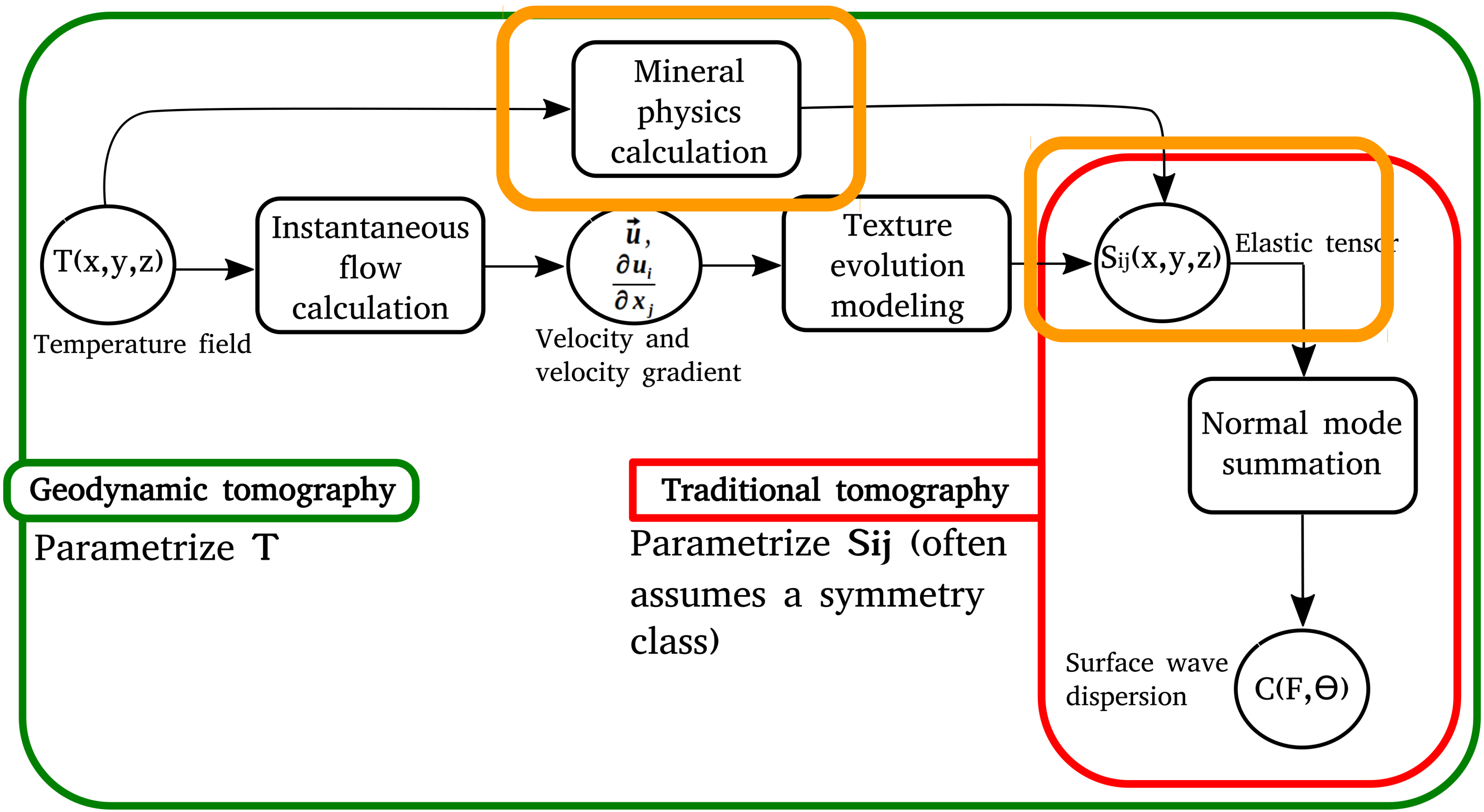

Joint geodynamic and seismic forward problem

Thermodynamic modeling of the isotropic component

- We model the **temperature and pressure dependence** of **isotropic P and S wave velocities** using the thermodynamic model of Stixrude and Lithgow-Bertelloni (2011).

- We scale the anisotropic tensor by taking the ratio between the shear moduli at a given T and P, and the shear moduli at reference T-P:

$$S(T,P)=S_0(T,P)+\frac{\mu(T,P)}{\mu(T_0,P_0)}\delta S(T_0,P_0)$$

Joint geodynamic and seismic forward problem

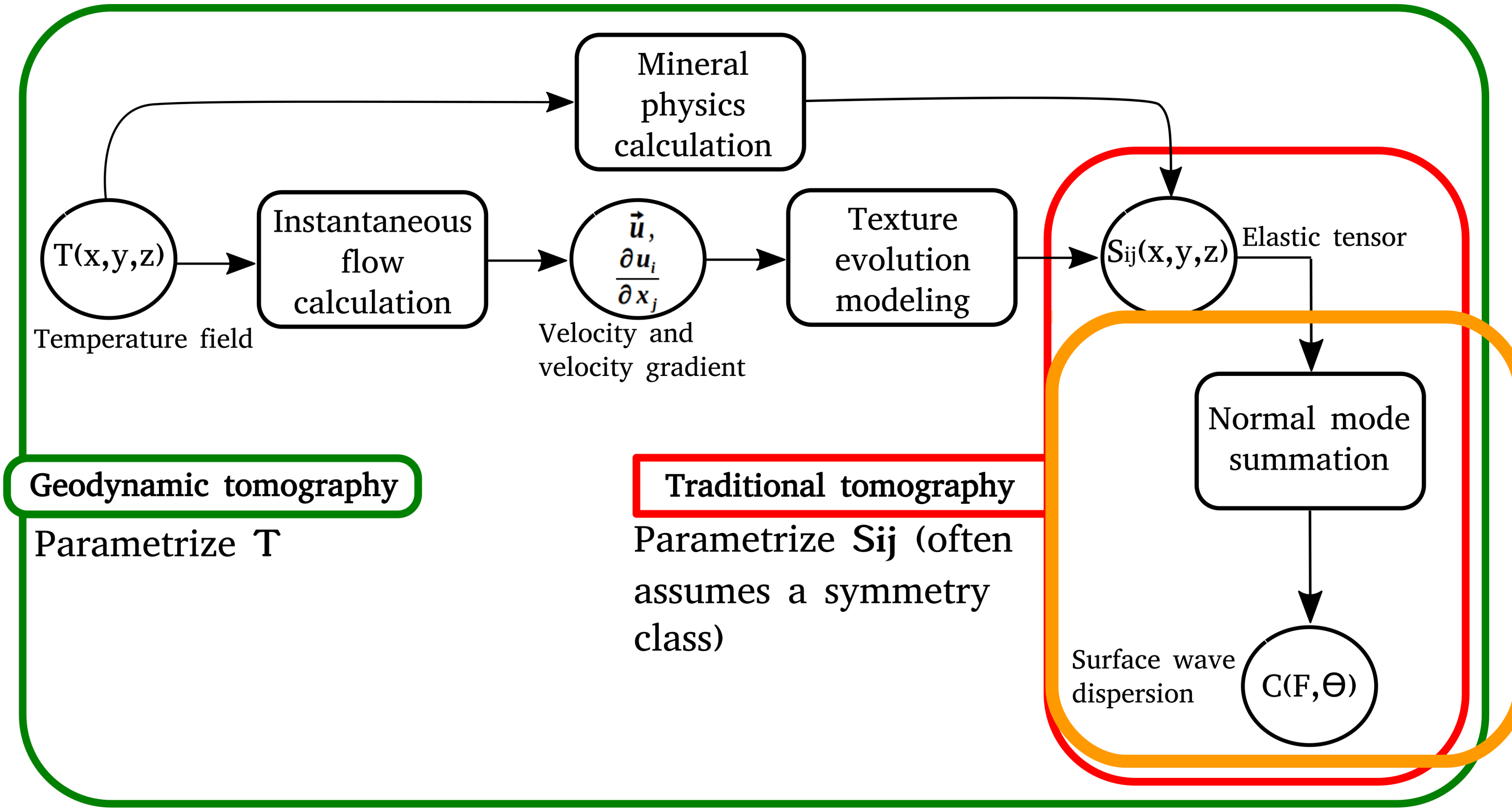

Joint geodynamic and seismic forward problem

In a weakly anisotropic medium, the phase velocity with azimuthal dependence follows the form:

$$\mathbf{c}(T,\theta) = \mathbf{c}_0(T) + \mathbf{c}_1(T)\cos(2\theta) + \mathbf{c}_2(T)\sin(2\theta)$$

Given the depth distribution of the 3-D elastic tensor **S**, we want to compute:

- Local surface wave dispersion curves at a given period, $\mathbf{c}_R$ and $\mathbf{c}_L$.
- Azimuthal variations, $\mathbf{c}_1$ and $\mathbf{c}_2$

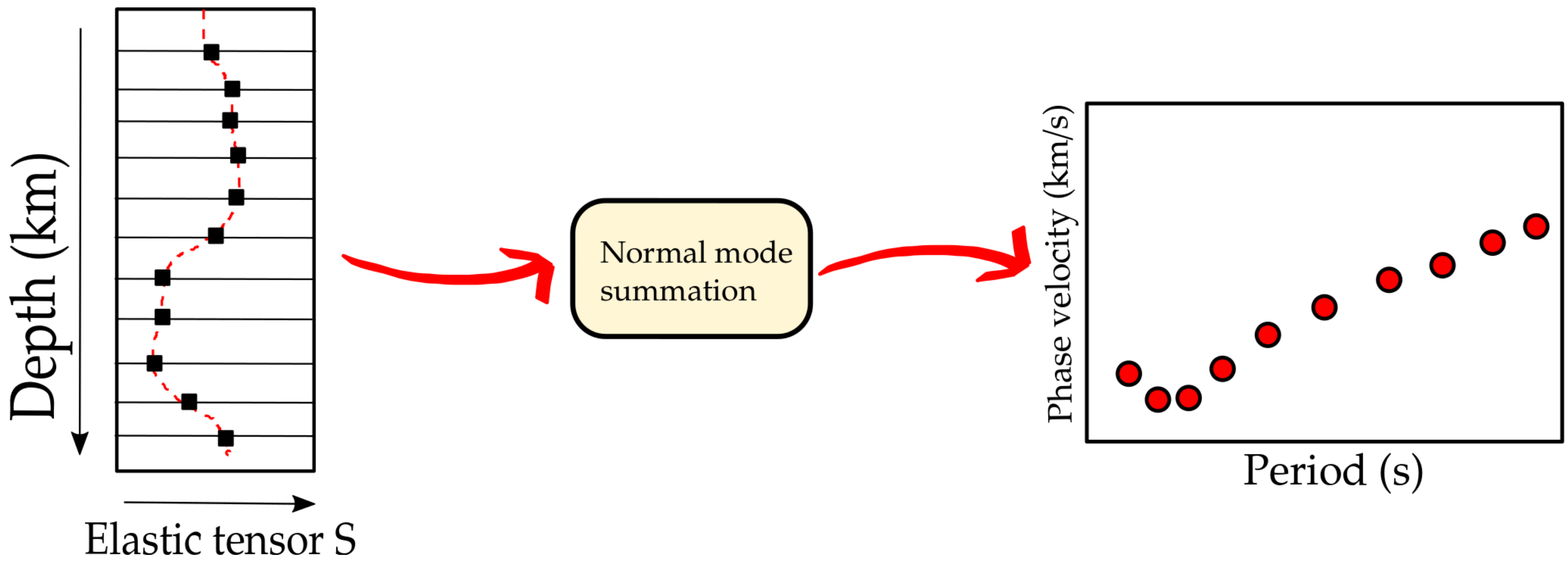

Bayesian inversion

The solution to the inverse problem is an ensemble of models cast in the form of a probability distribution called the **posterior.**

Baye's Theorem

Posterior ≈ Likelihood x Prior

$$p(\underset{1}{m}|\underset{2}{d}) \approx \underbrace{p(d|m)}_{3}\,\underbrace{p(m)}_{4}$$

1. Model: Temperature field and activation energy for viscosity.

2. Data: Surface wave dispersion measurements.

3. Likelihood: Level of data fit.

$$p(d|m) = \frac{1}{2\pi\sigma^{N/2}} \exp\left[\frac{-\|d-g(m)\|}{2\sigma^2}\right]$$

4. Prior: Preexisting information.

$$p(m_i) = \begin{cases} 0 & m_i > m_{\max},\ m_i < m_{\min} \\ \frac{1}{\Delta m} & m_{\min} \le m_i \le m_{\max} \end{cases}$$

Random walk approach to sample the posterior distribution

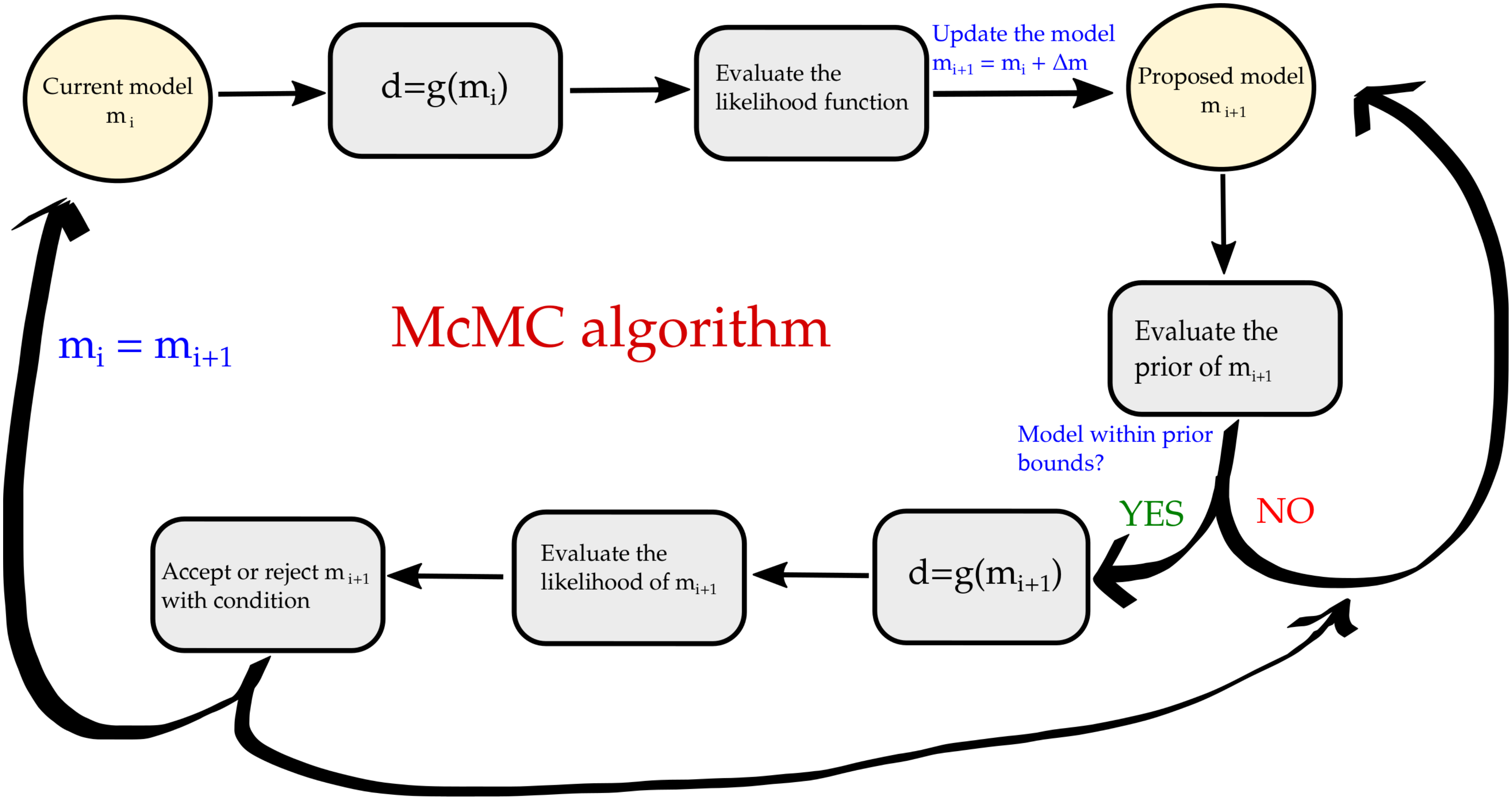

Inversion tests

Generating the synthetic data

- Consists of Rayleigh $\mathbf{c}_R$ and Love dispersion curves $\mathbf{c}_L$, and azimuthal variations $\mathbf{c}_1$ and $\mathbf{c}_2$ at one of the 16 geographical locations (specified by ▼) .
- **Observed data**:
  - Generated from D-Rex (i.e true model).
  - Corrupted with random uncorrelated noise (Gaussian)
- **Estimated data**: Generated from neural networks (i.e. inversion).

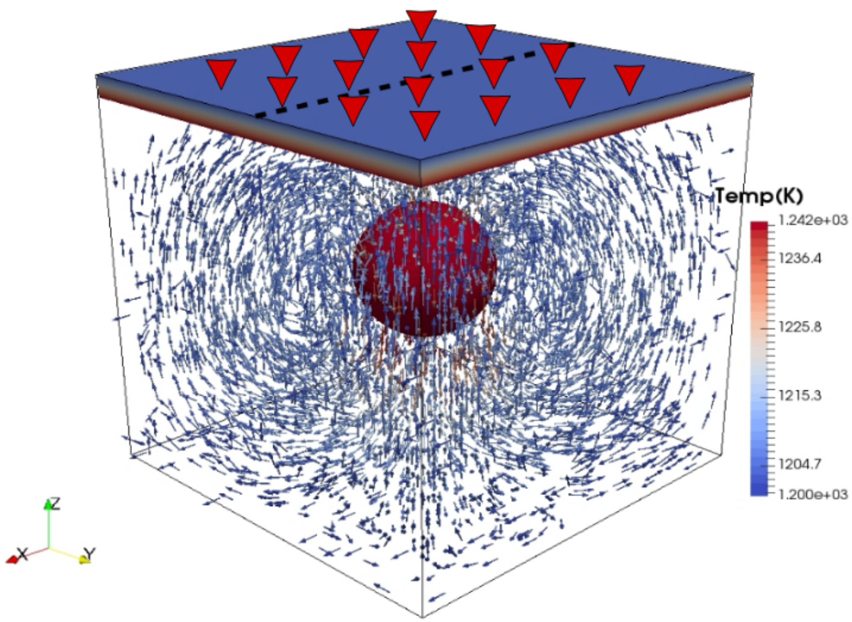

Each location contains dispersion measurements generated by a 3-D deforming upper-mantle.

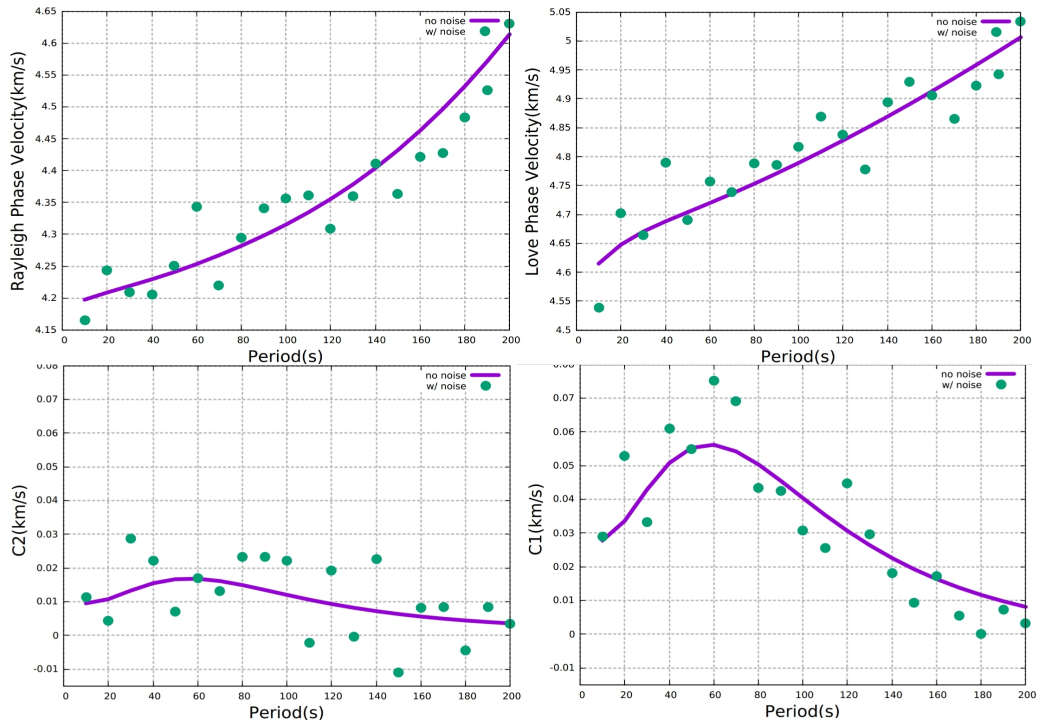

Observed data with and without added noise at a given location ($\sigma_{R,L}$=0.05 km s^{-1}, $\sigma_{1,2}$=0.01 km s^{-1})

Inversion tests

Isotropic versus anisotropic inversion

Isotropic inversion:

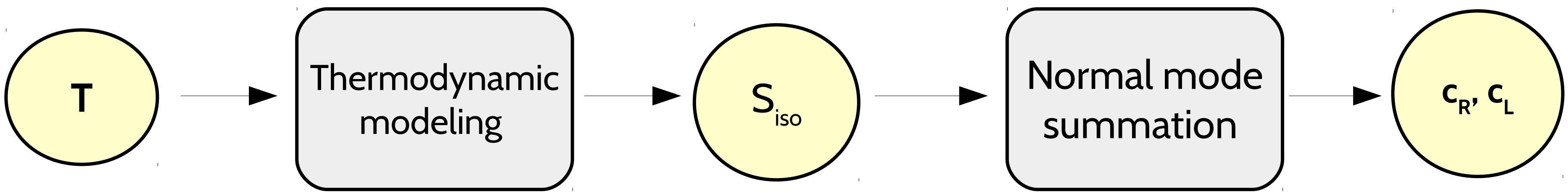

Anisotropic inversion:

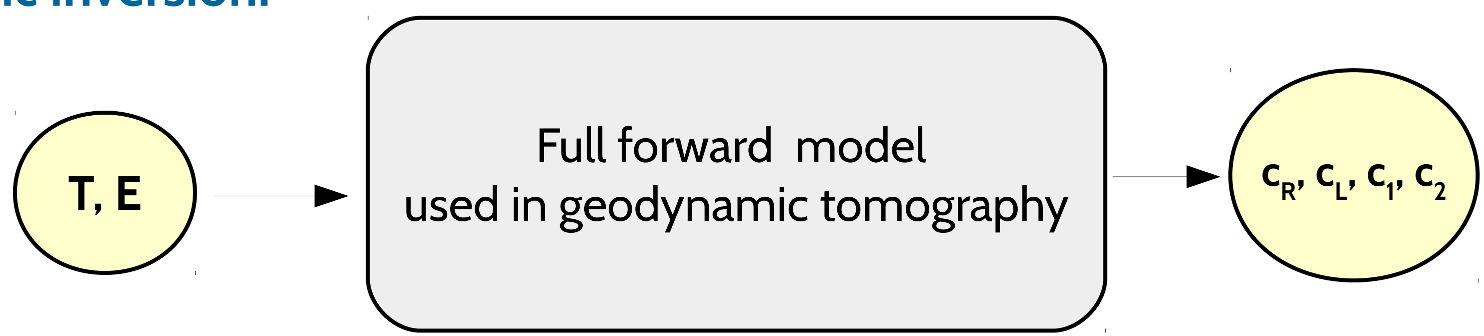

Inversion tests

Inverting one spherical anomaly

Model setup

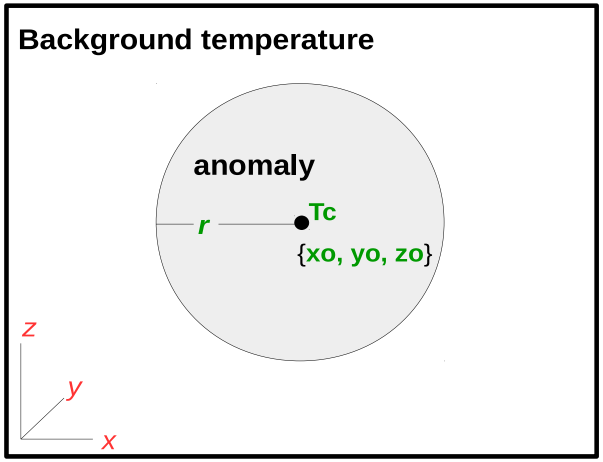

Temperature field - the model

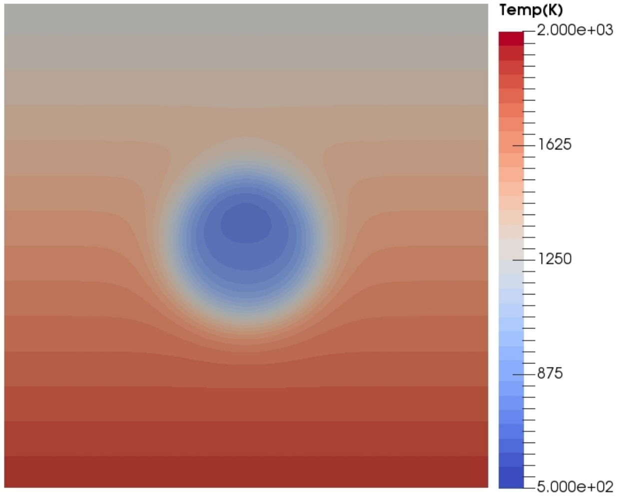

True model parameters

Model parameter	Assigned value
x_0	200 km
y_0	200 km
z_0	200 km
R	120 km
T_c	800 K
E	11.0

Inversion tests

Inverting one spherical anomaly - results

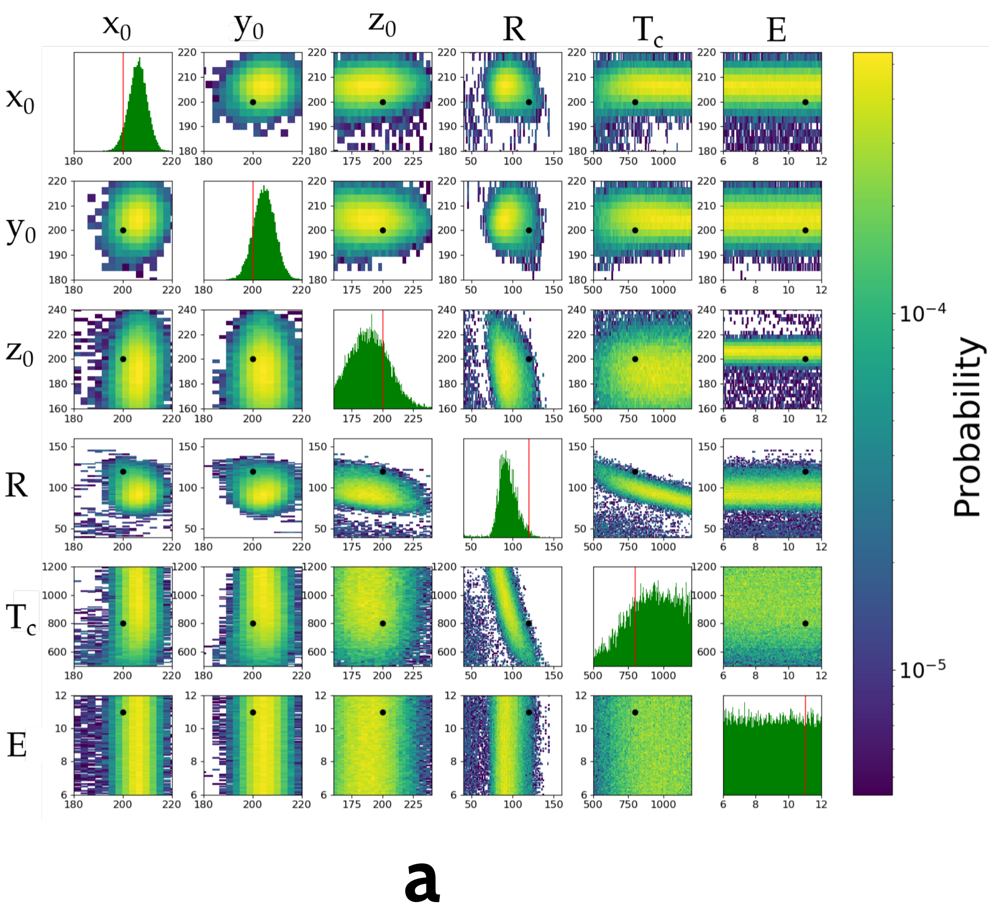

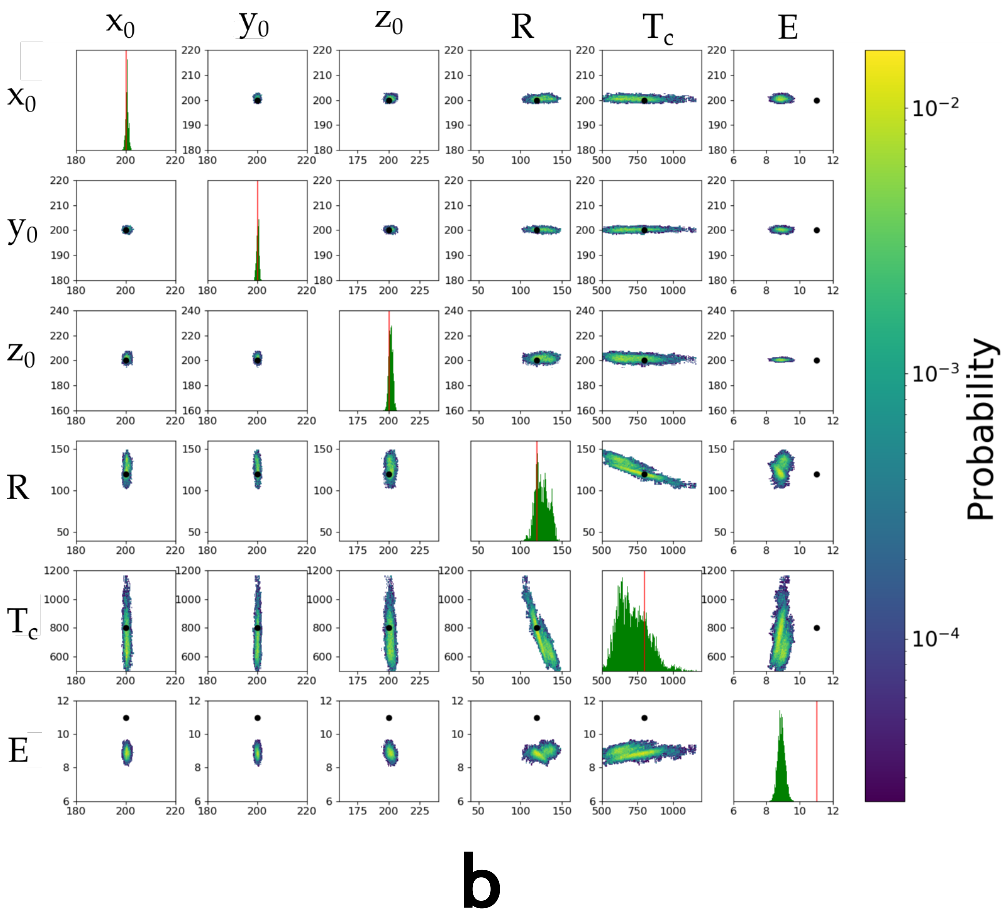

Posterior probability distribution in the 6-D parameter space inferred from:
a. isotropic inversion,
b. anisotropic inversion

Inversion tests

Inverting one spherical anomaly - results

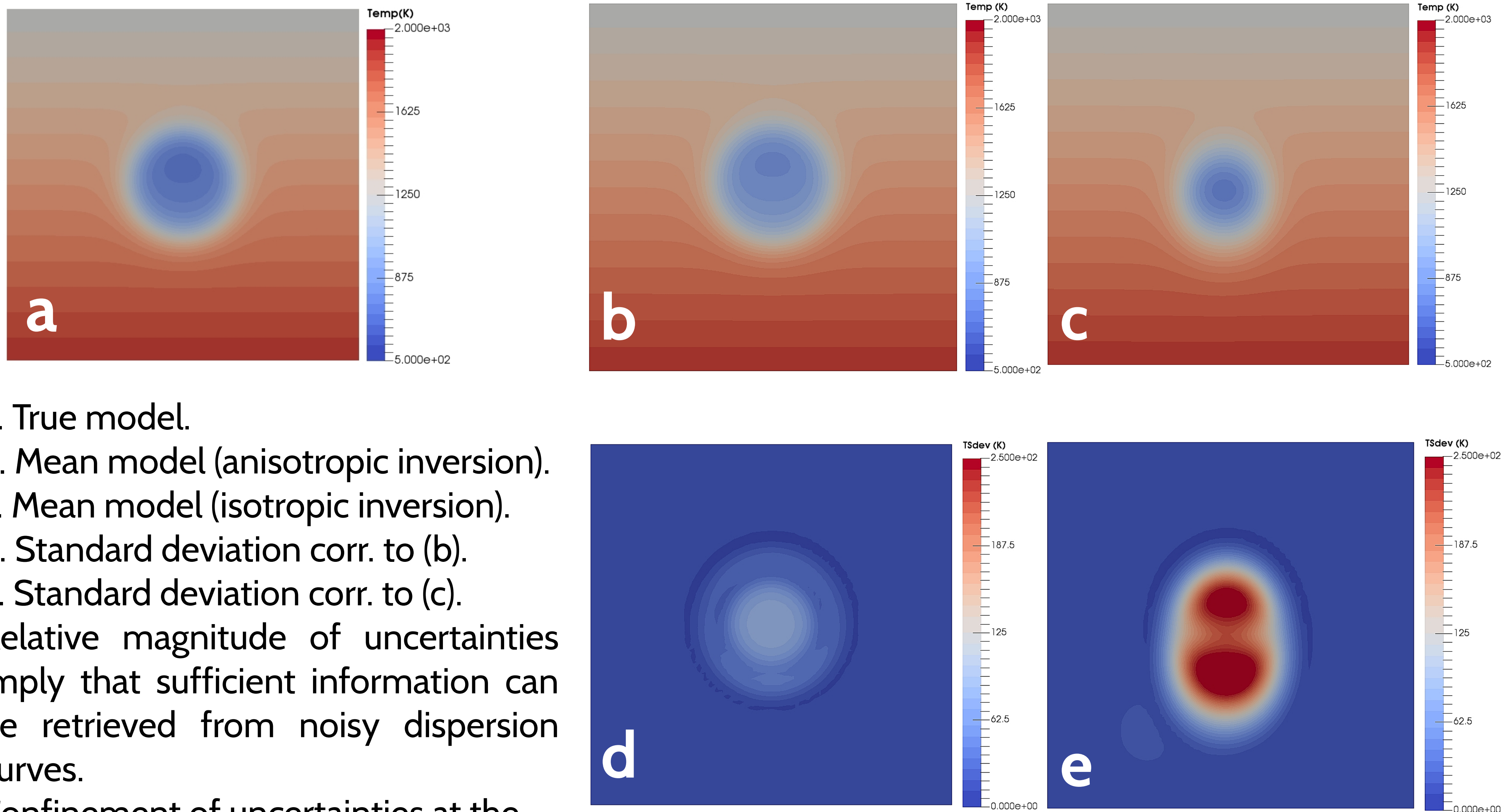

- a. True model.
- b. Mean model (anisotropic inversion).
- c. Mean model (isotropic inversion).
- d. Standard deviation corr. to (b).
- e. Standard deviation corr. to (c).
- Relative magnitude of uncertainties imply that sufficient information can be retrieved from noisy dispersion curves.
- Confinement of uncertainties at the center imply convergence.

Inversion tests

Inverting one spherical anomaly - results

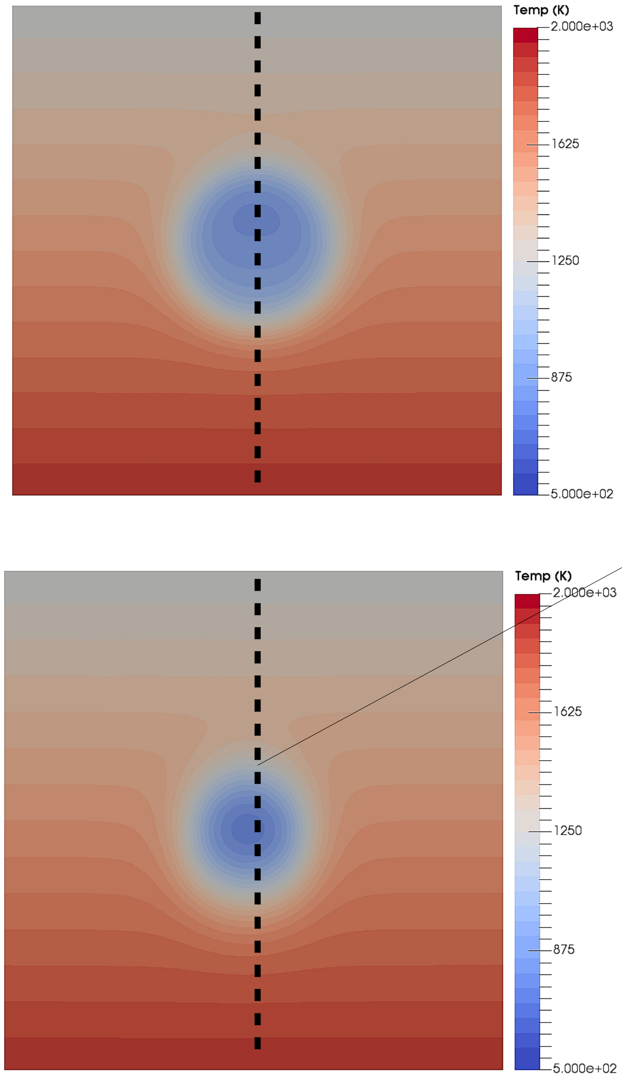

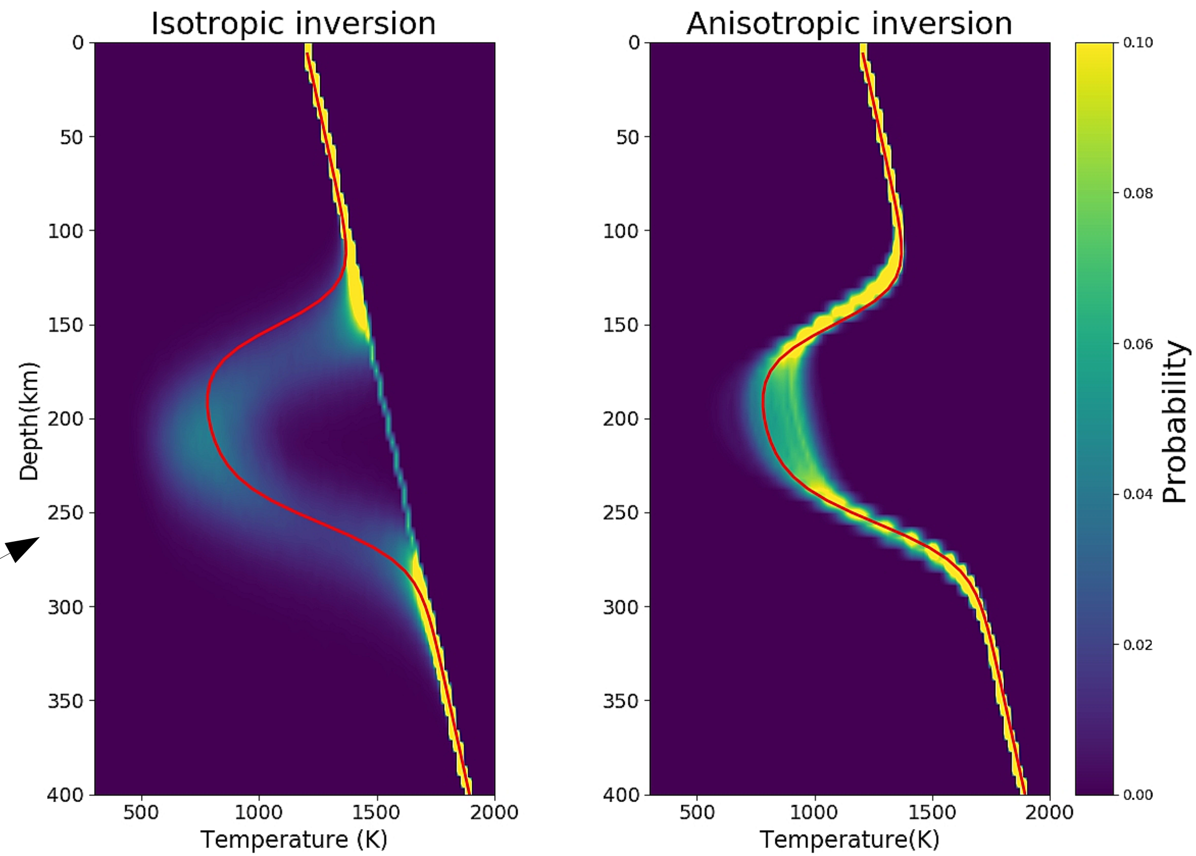

1-D depth posterior probability profiles of temperature resulting from the two methods.

Inversion tests

Inverting one spherical anomaly - results

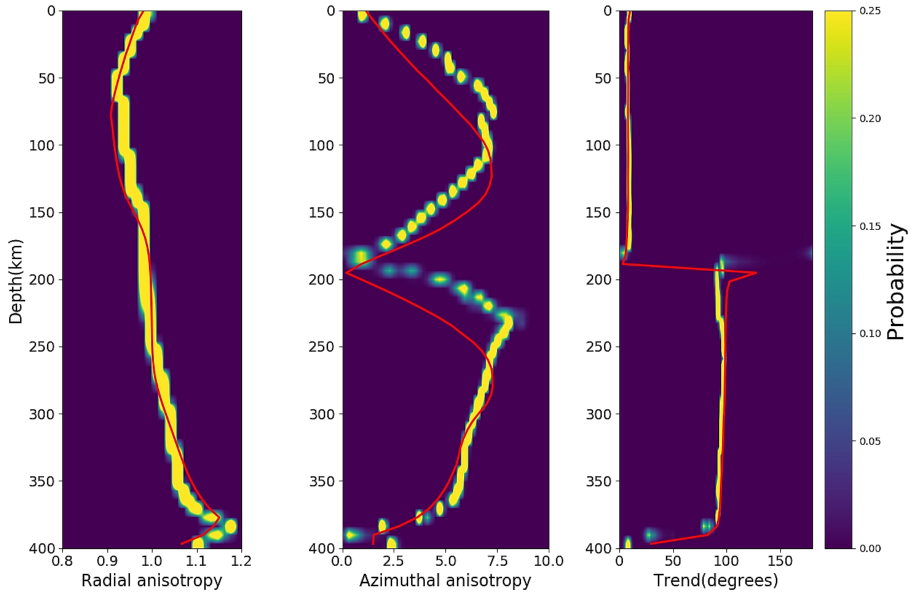

1-D depth posterior probability profiles of radial anisotropy, azimuthal anisotropy, and the azimuthal angle.

Since the elastic tensor is implicitly computed everywhere, geodynamic tomography offers the capability to constrain both radial and azimuthal anisotropy.

Total anisotropy | Radial anisotropy

True model

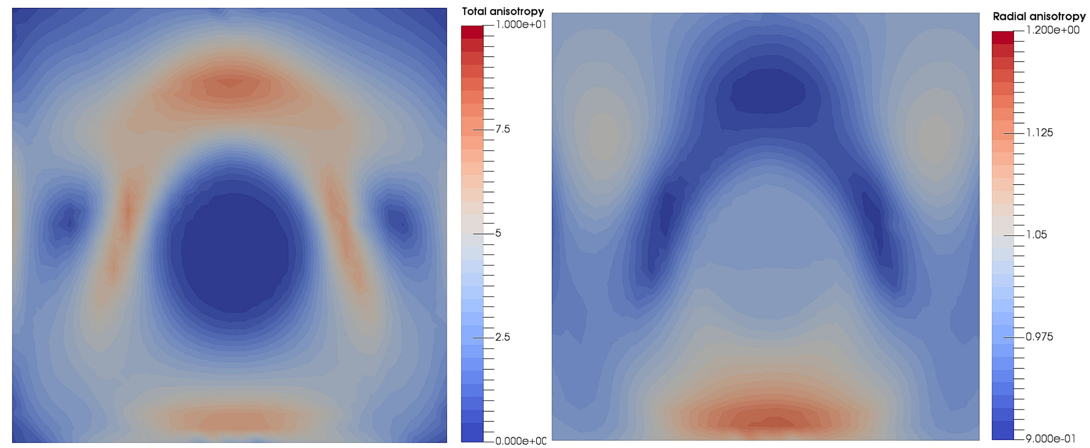

Inverted model

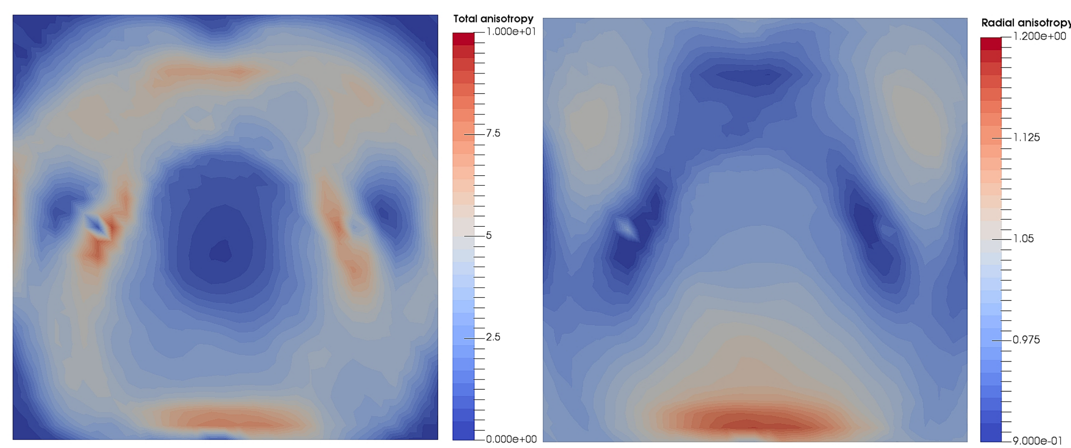

Inversion tests

Inverting multiple spherical anomalies - results

1-D depth posterior probability profiles at a given location

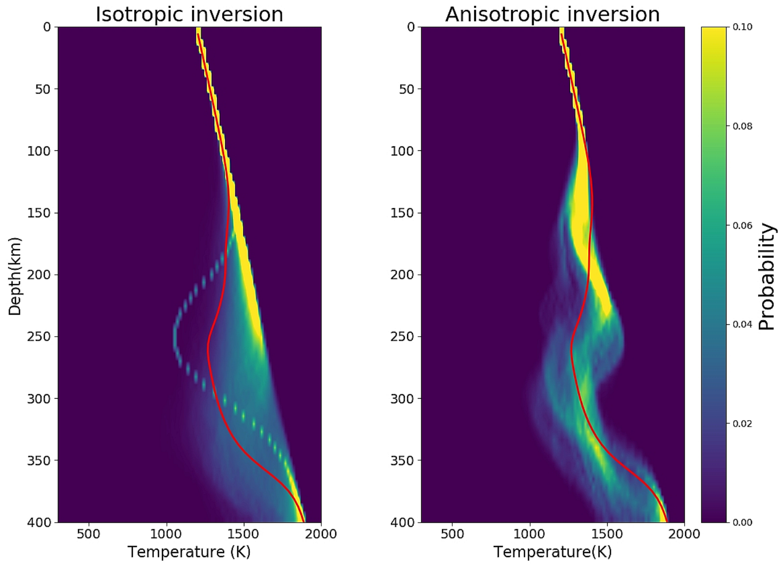

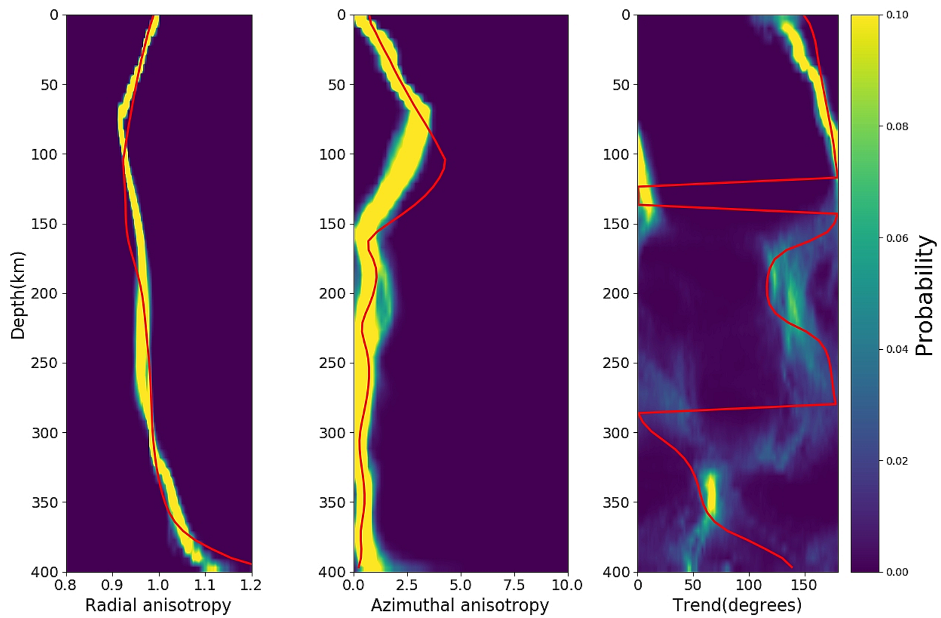

True and mean temperature fields

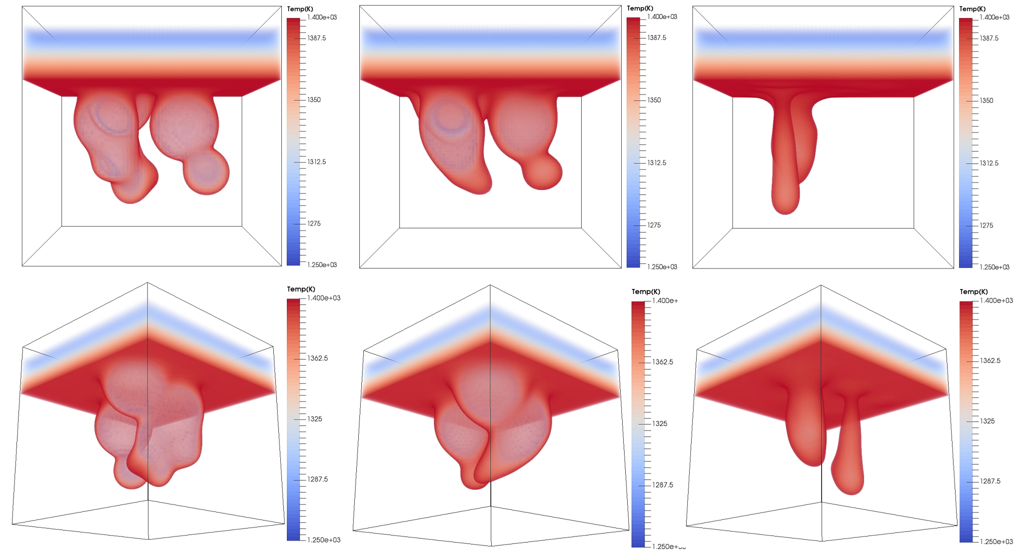

Standard deviation

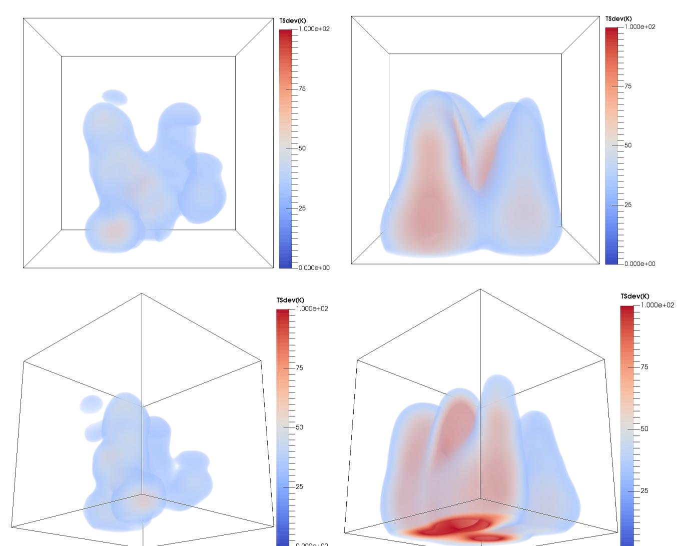

Inversion tests

Application to instantaneous flows induced by subduction

Model setup

- Five unknown parameters:
  - Dip angle θ, slab length L, thickness R
  - Temperature T_C
  - Activation energy E

Temperature

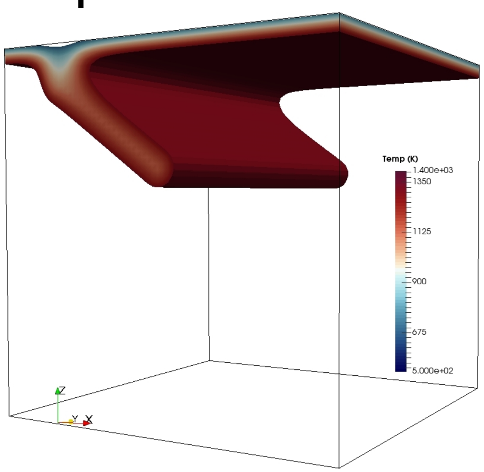

Model parameter	Assigned value
L	150 km
R	120 km
θ	35^0
T_c	800 K
E	11.0

Flow field

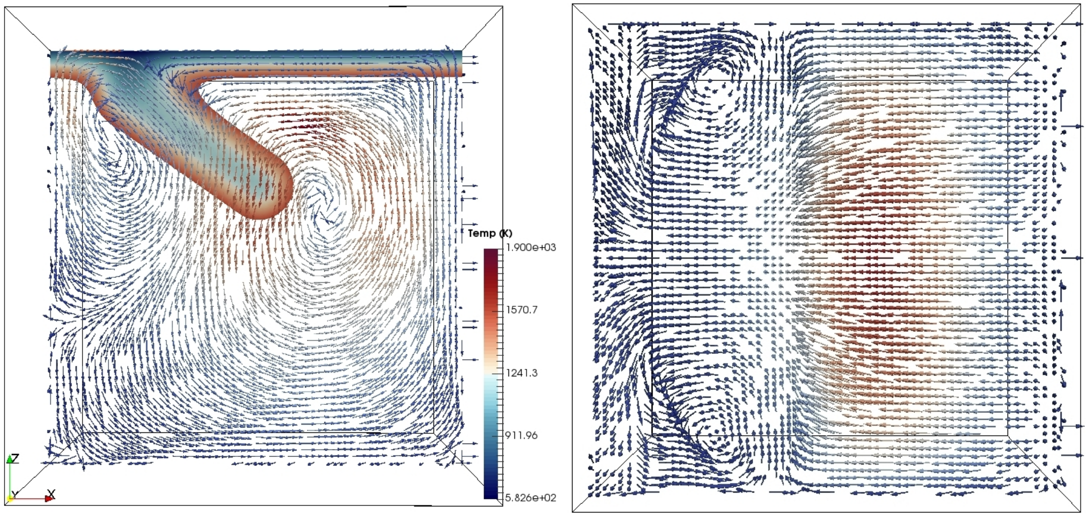

Dispersion measurements with and without noise

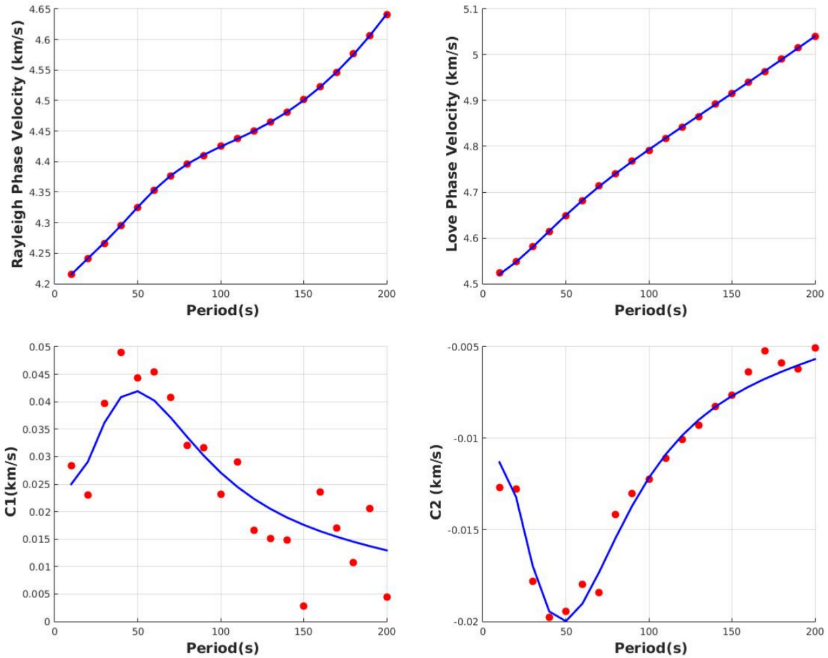

Data: Surface wave dispersion measurements with random uncorrelated noise but much smaller ($\sigma_{R,L}$=0.001 km s^{-1}, $\sigma_{1,2}$=0.005 km s^{-1}).

Inversion tests

Application to instantaneous flows induced by subduction

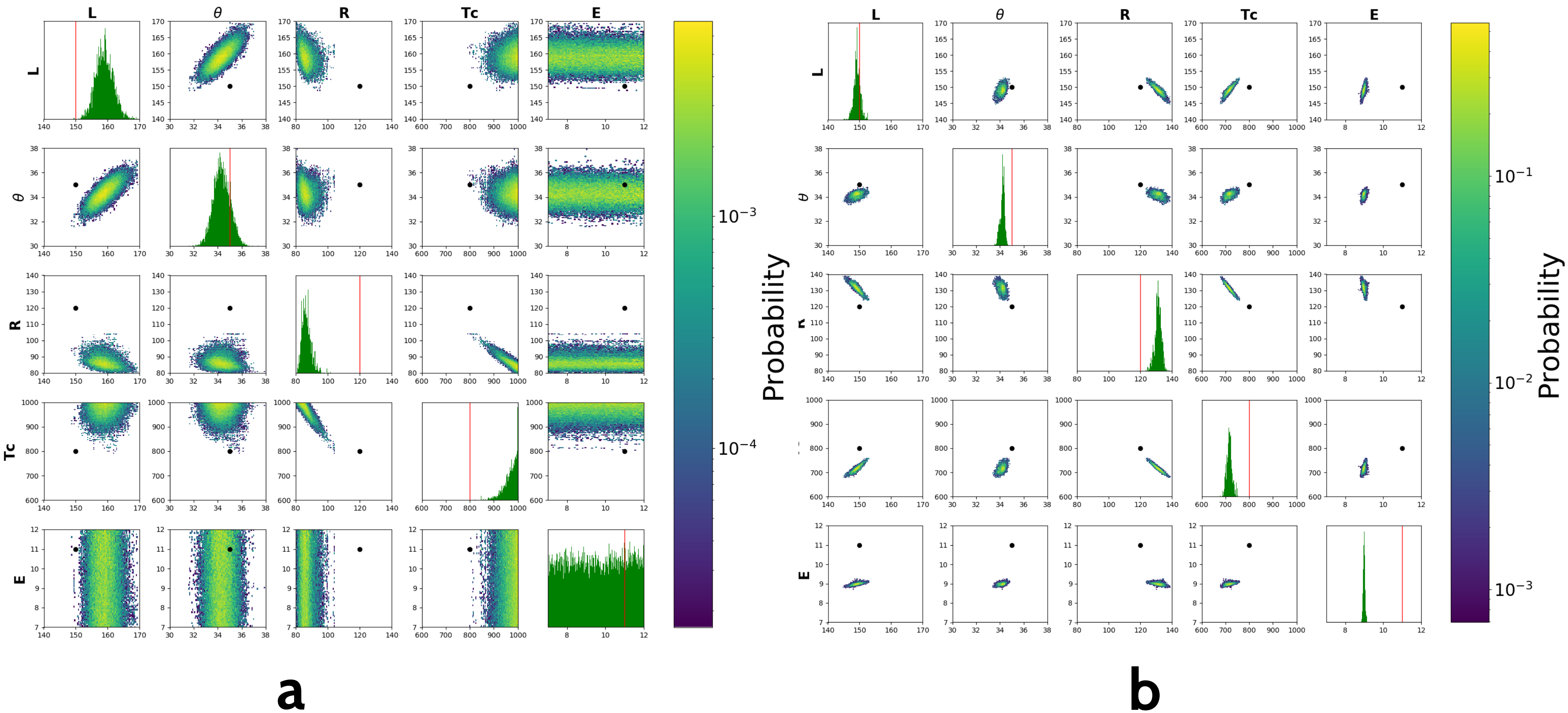

Posterior probability distribution in the 6-D parameter space inferred from:
a. isotropic inversion,
b. anisotropic inversion

Inversion tests

Application to instantaneous flows induced by subduction

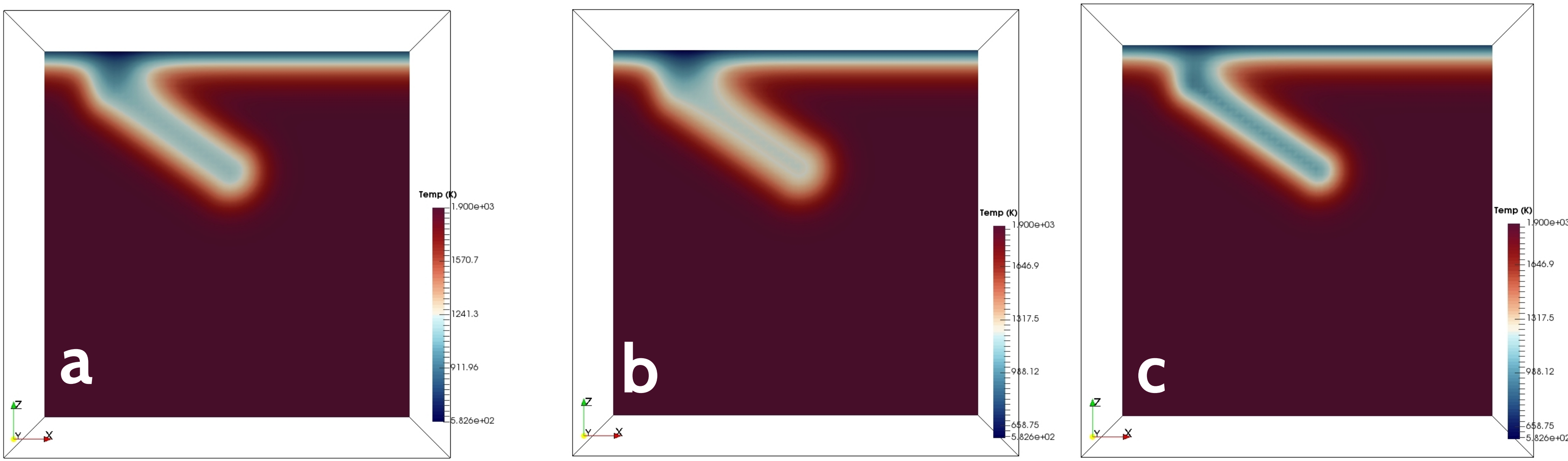

- a. True model.
- b. Mean model (anisotropic inversion).
- c. Mean model (isotropic inversion).
- d. Standard deviation corr. to (b).
- e. Standard deviation corr. to (c).
- Due to low noise levels, anisotropy is not as beneficial in the recovery of the structures.

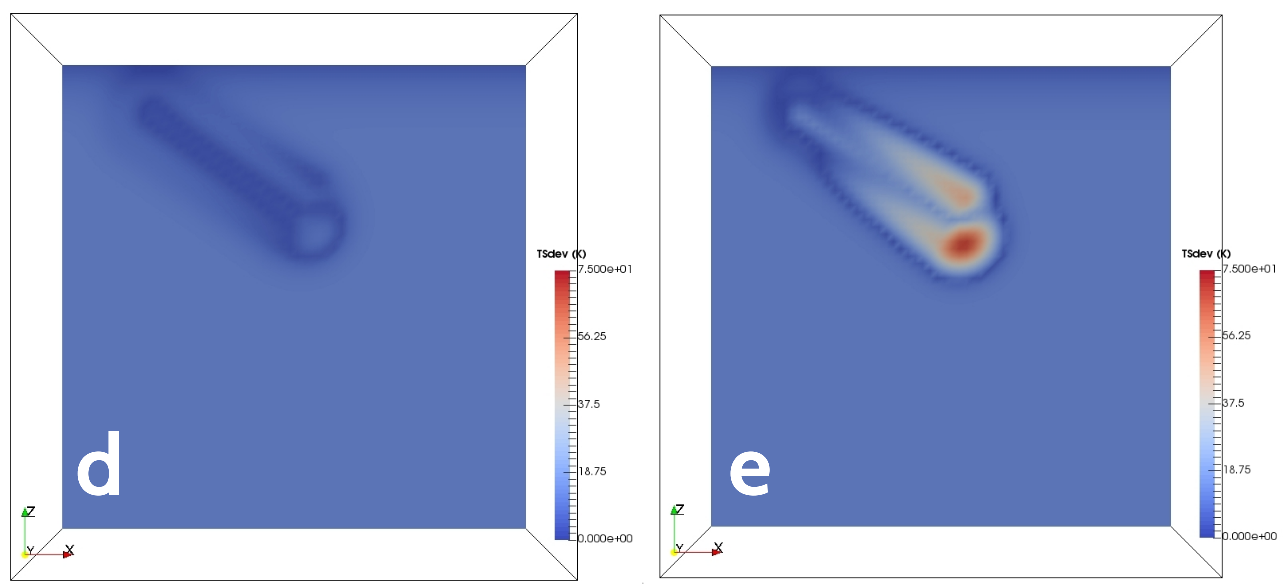

Inversion tests

Application to instantaneous flows induced by subduction

1-D depth posterior probability profiles at a given location

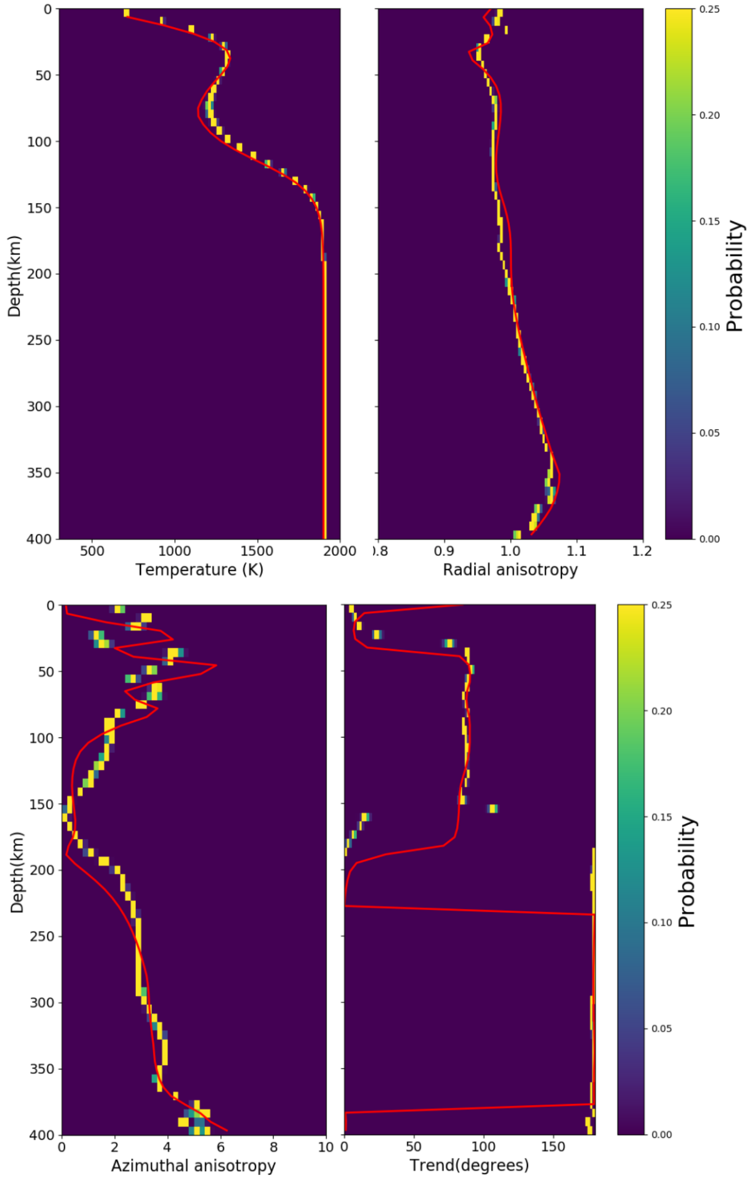

Total anisotropy

Radial anisotropy

True model

Inverted model

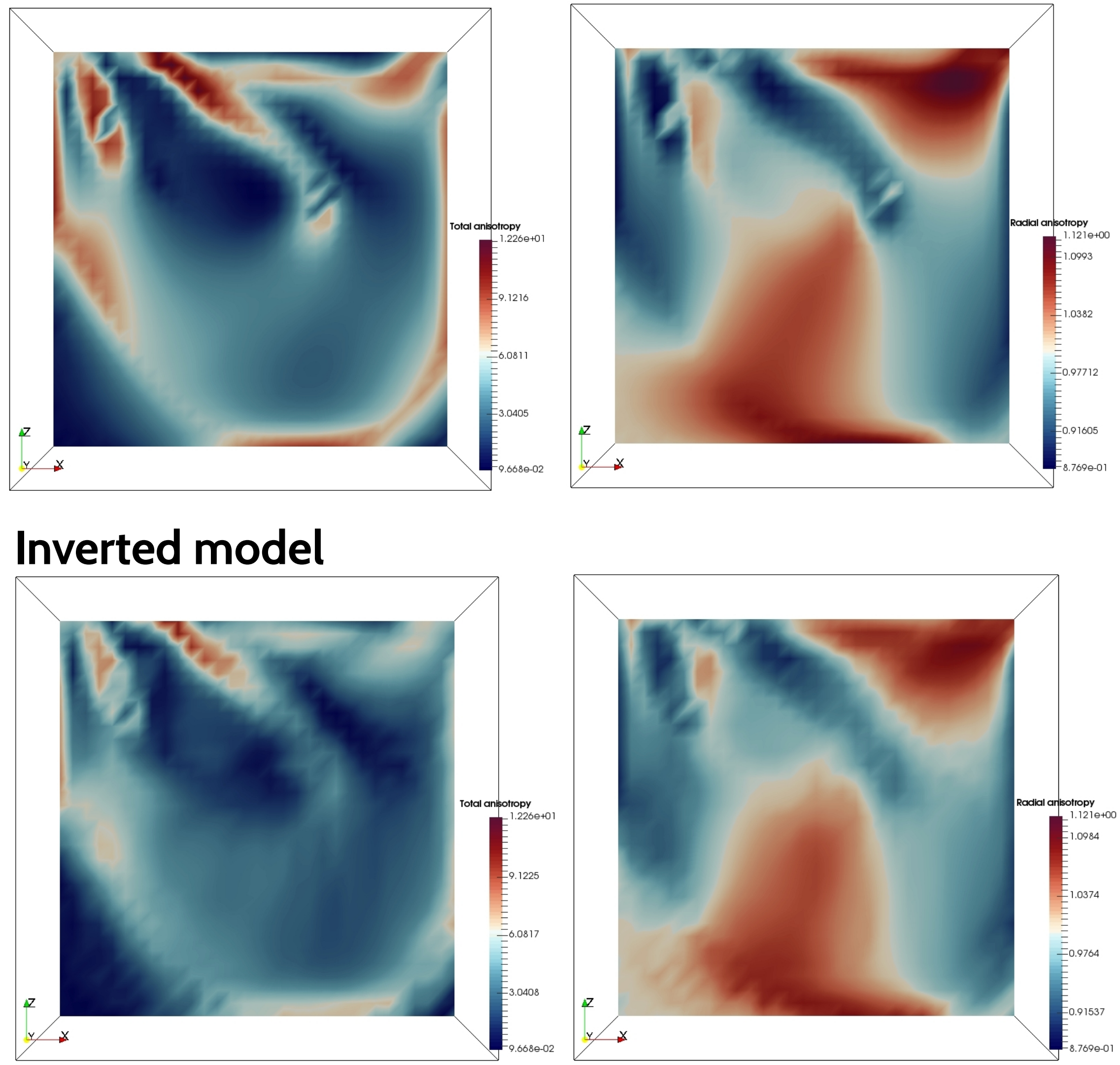

Conclusion

- We developed **geodynamic tomography**, a novel approach to the tomographic problem by incorporating constraints from **geodynamic** and **mineral physics** modeling.

- It possesses the following key advantages:
  - **Reduces the number of Earth models** to a subset consistent with **geodynamic predictions**.
  - **Recovers the complete deformation patterns** from surface wave data alone.
  - Resolves some long-standing issues in surface wave tomography:
    - Ability to **resolve the elastic tensor** everywhere.
    - **Reduction** of the amount of **free parameters**.

- Cast in a Bayesian framework, we demonstrated that any implicitly computed variable can be formulated in their own probability distribution.

- Along the process, we have implemented a quick method to compute seismic anisotropy. This opens new doors for a class of surrogate models that could accommodate any types of flow.

Conclusion

Limitations

- Random uncorrelated errors.

- Adapting to other data-types
  - ➔ Gravity anomalies
  - ➔ Surface topography
  - ➔ Surface velocities

- Physical assumptions imposed
  - ➔ Nature of the flow model
  - ➔ Composition of the mantle

- Anisotropy is purely intrinsic
  - ➔ Finite-frequency seismic data maps small-scales into large-scale anisotropy (SPO).
  - ➔ Anisotropy from tomography: Intrinsic or extrinsic origin?

$$\xi^{*} = \xi_{SPO}\,\xi^{*}_{CPO}$$

Extrinsic radial anisotropy can be extracted from a tomographic model (*Magali, et. al. 2021, Submitted to JGR*).

Conclusion

Potential application to a real-Earth problem

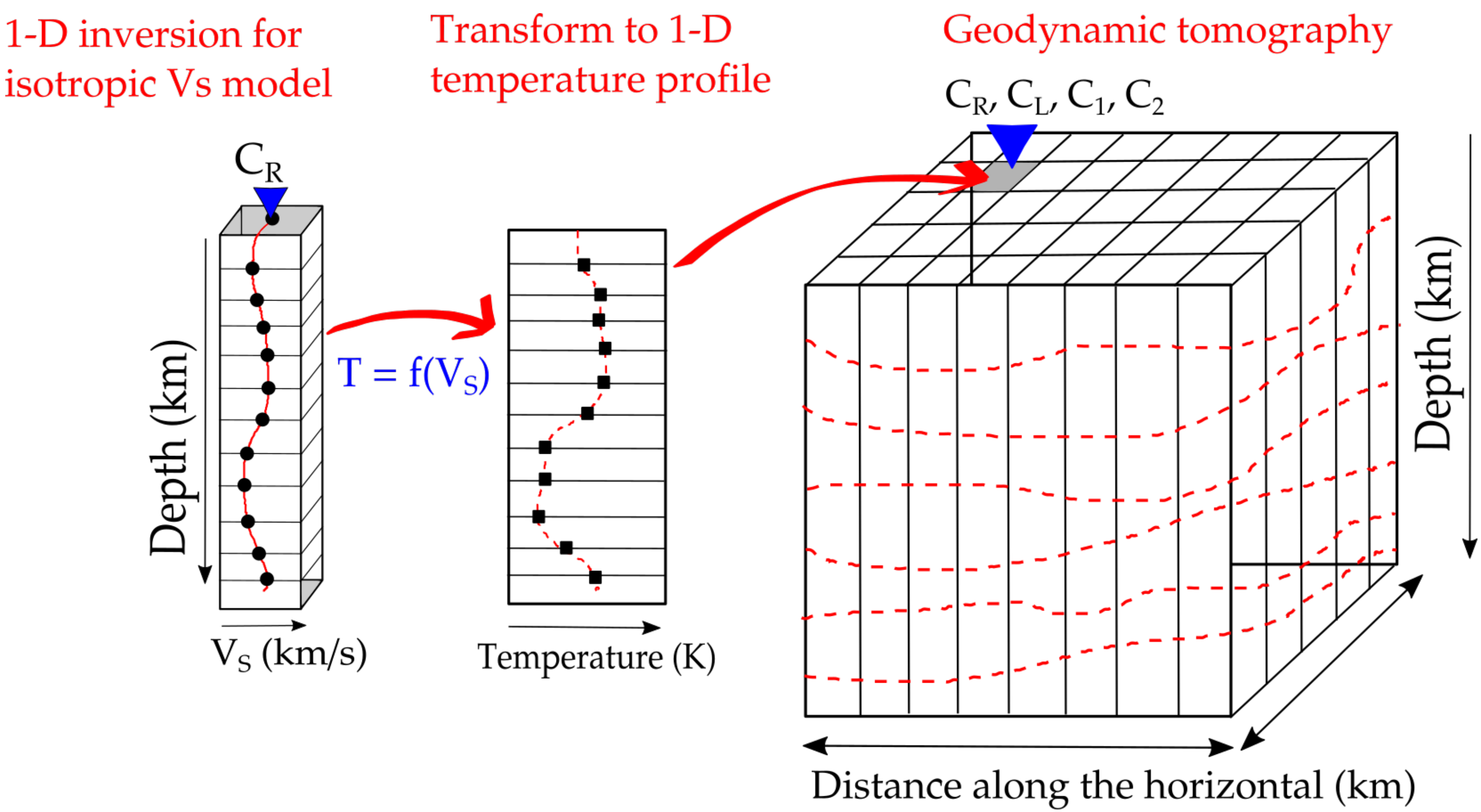

Three-step approach to geodynamic tomography.